Mitglied der Helmholtz-Gemeinschaft

Werkstoffentwicklung für die elektrochemische Energietechnik

Olivier Guillon

Institute of Energy and Climate Research
IEK-1: Materials Synthesis and Processing

HELMHOLTZ ASSOCIATION


Energy


Earth & Environment

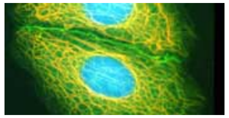
Health

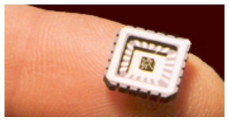
Key Technologies

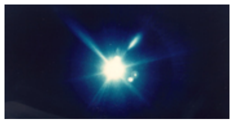
Structure of Matter


Transport & Space

18 Centers

Budget: € 4.45 billion per annum

38,700 members of staff

Forschungszentrum Jülich: Facts and Figures

People	Budget	Science

People

- Employees: 5.787
- 900+ guest scientists (>45 countries)

Budget

- Budget: 552 Mio €
- Third-party funding: ~ 197 Mio €

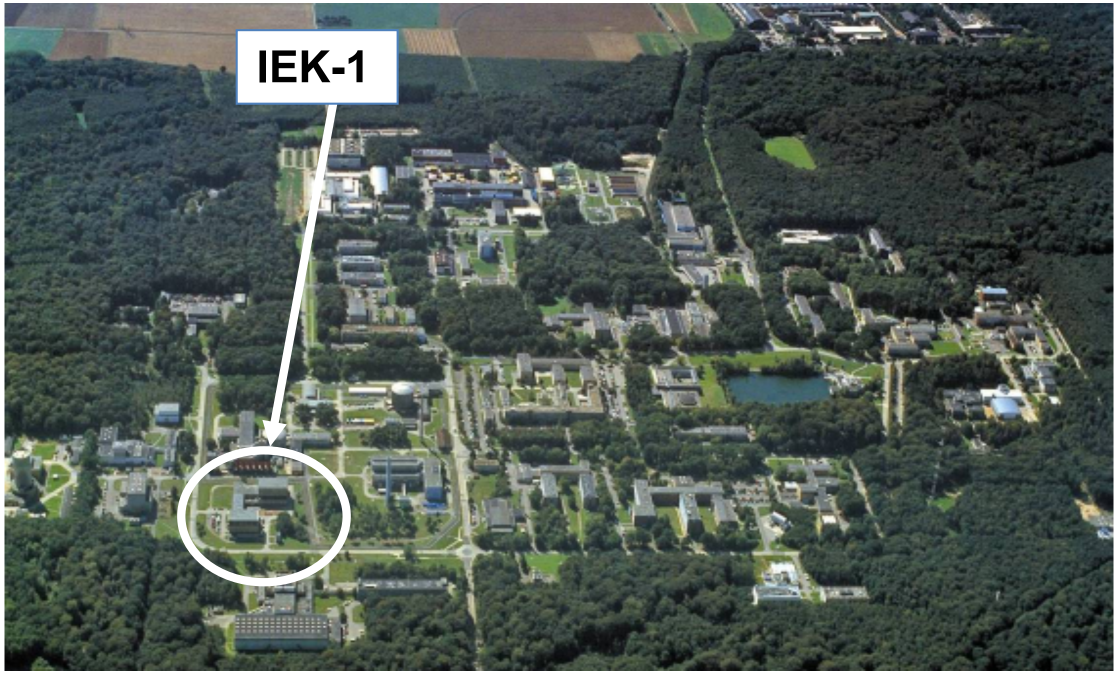

Science

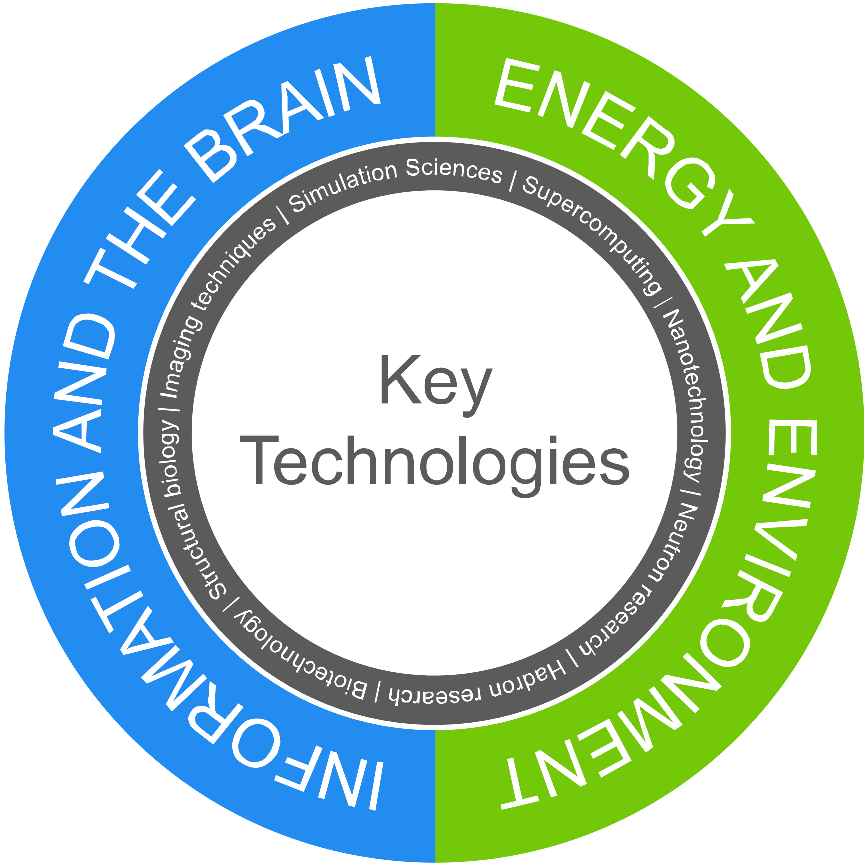

Institute of Energy and Climate Research

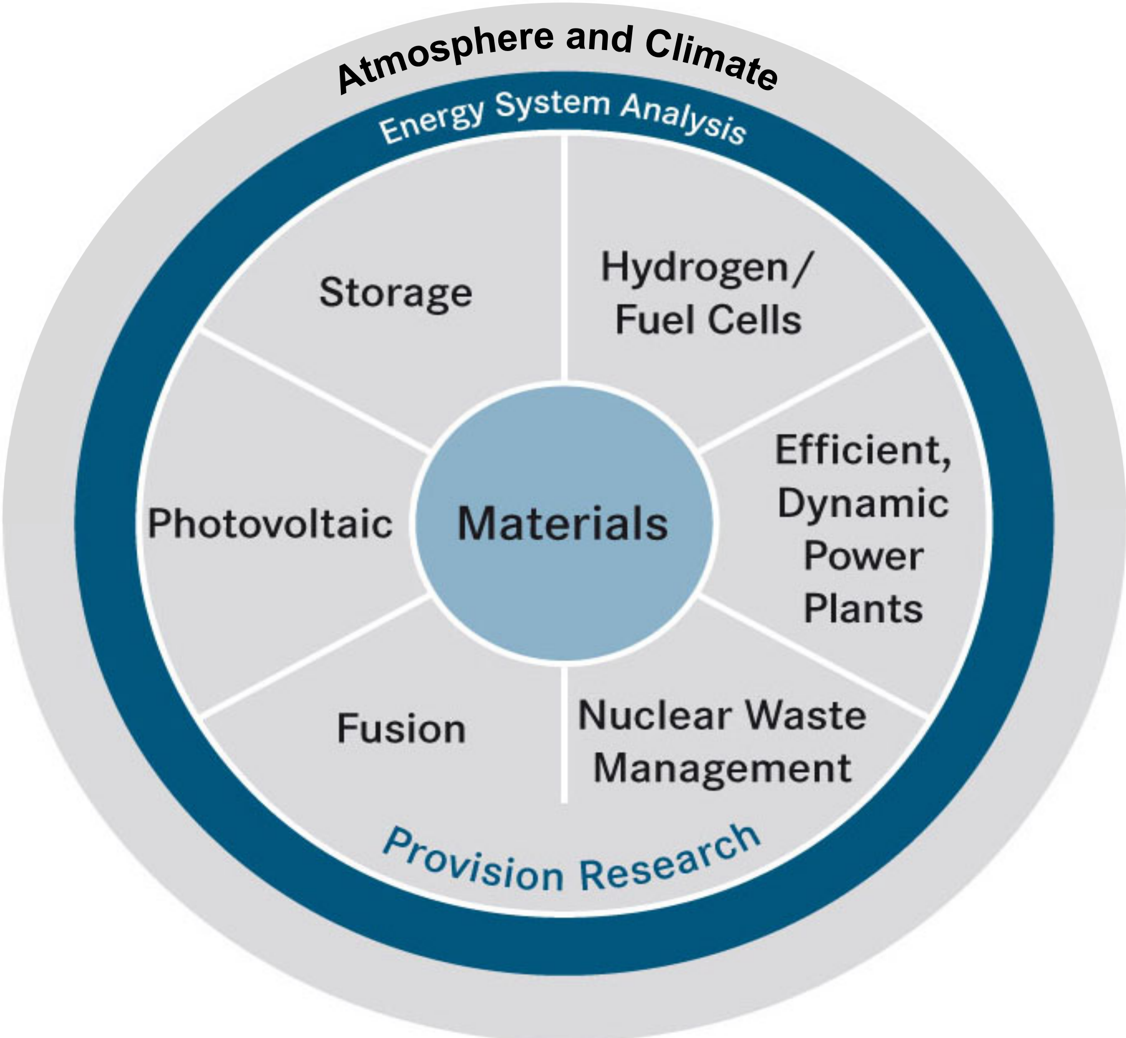

882 Staff

634 Energy Research

99 Climate Research

149 PhD Students:
Helmholtz Graduate school

Helmholtz Interdisciplinary Doctoral Training in Energy and Climate:
HITEC

Materials Research as Core Competence

Challenges related to the Energiewende

‚Energiewende' objectives with rising share of renewable energies:

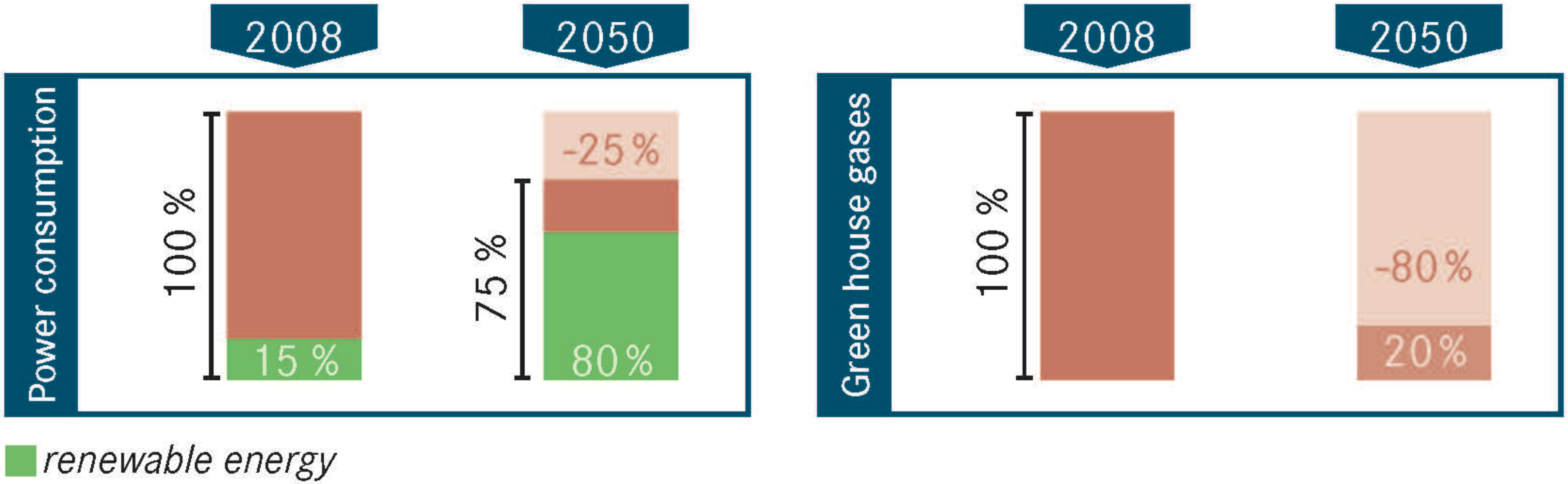

Matching fluctuating availability of renewable energy to demand requires versatile storage options and coupling of different energy carriers

Challenges related to the Energiewende

Balancing volatile power generation and demand
to secure supply stability

→ **Need for storage underestimated!**

Generation of photovoltaic and wind power in Germany in 2013:

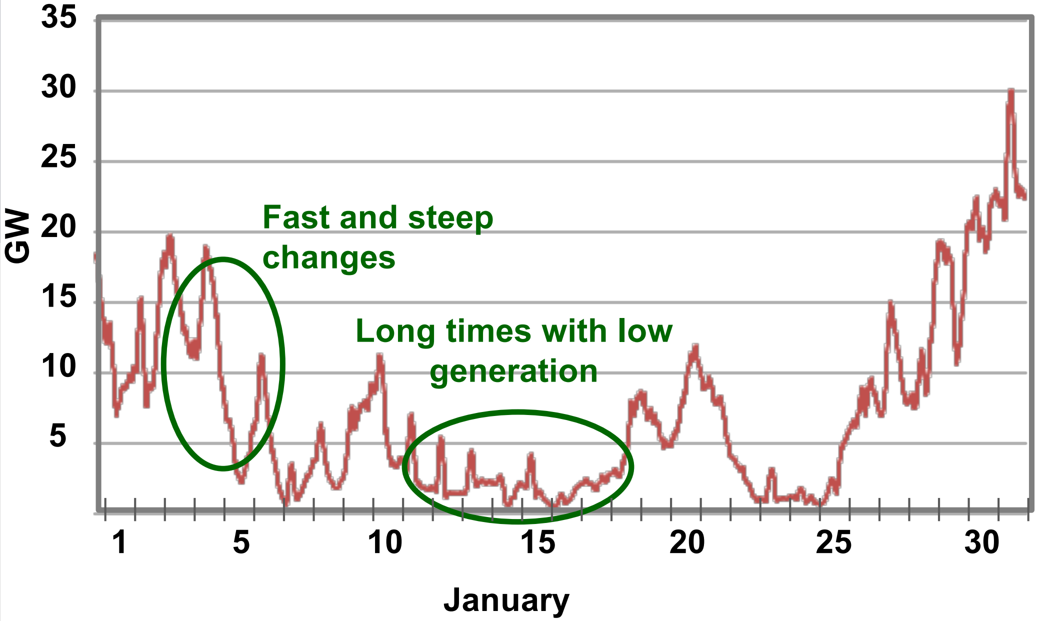

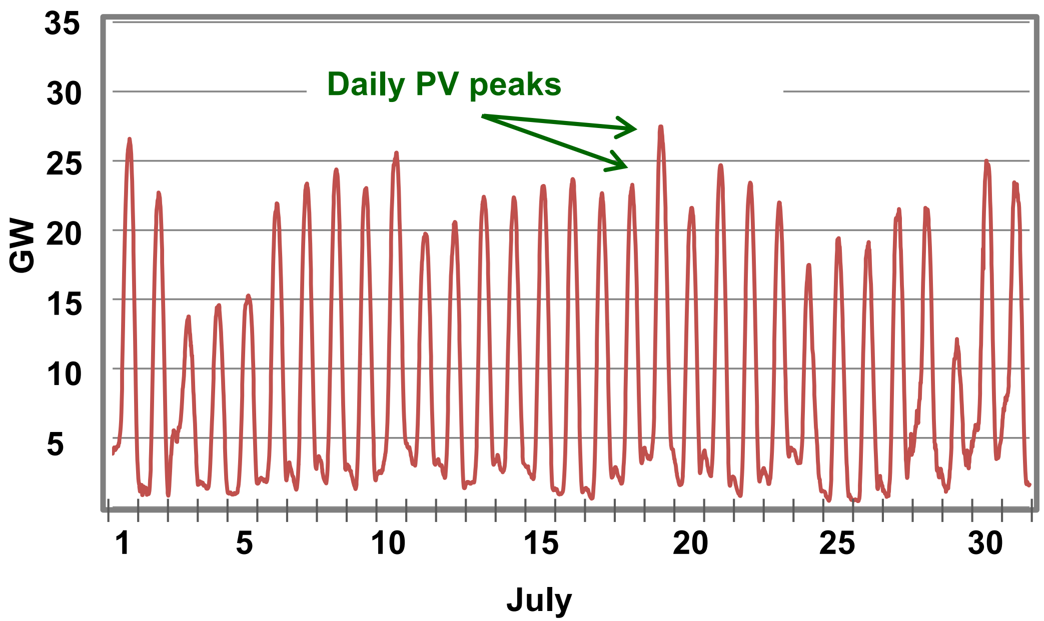

(Data from transmission system operators)

Challenges related to the Energiewende

Chemical energy for storage on different time scales and various use cases

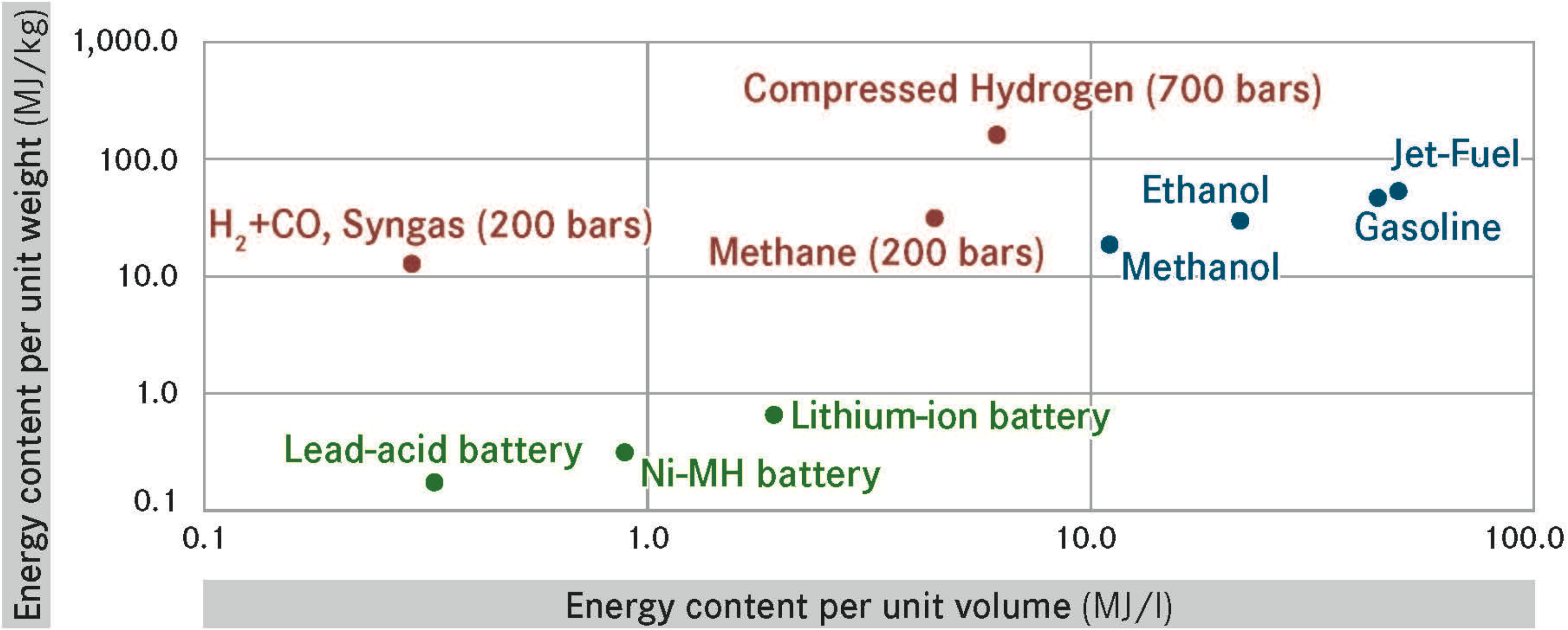

Liquid energy carriers: easy handling, storage and transport

IEK-1 at a glance

From raw material to component:
- Development of functional materials
  (ionic and electronic conductors, thermo-mechanically stable layers)
- Processing of multilayered systems

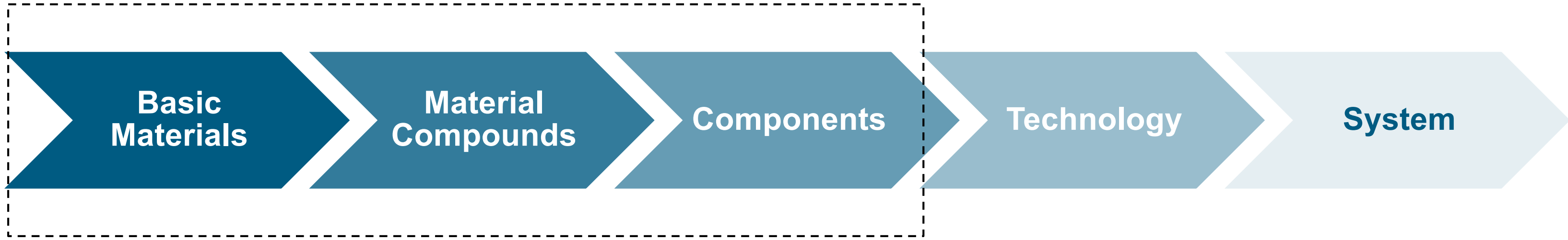

High-temperature materials and coatings

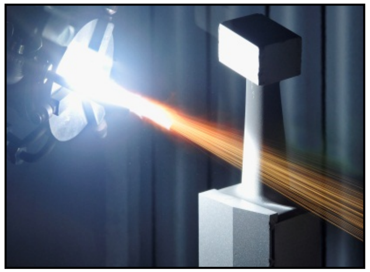

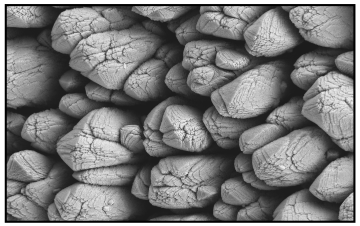

Gas separation and reactor membranes

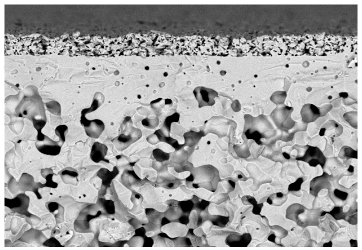

Solid Oxide Fuel Electrolysis Cells

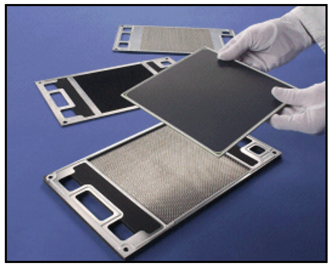

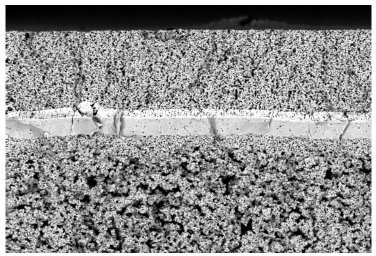

Solid-state Batteries

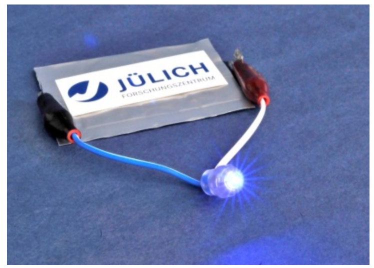

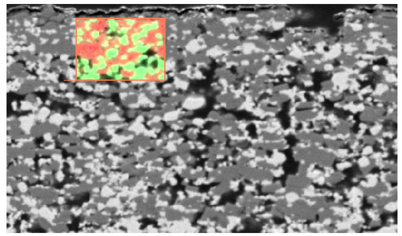

IEK-1 at a Glance: Processing

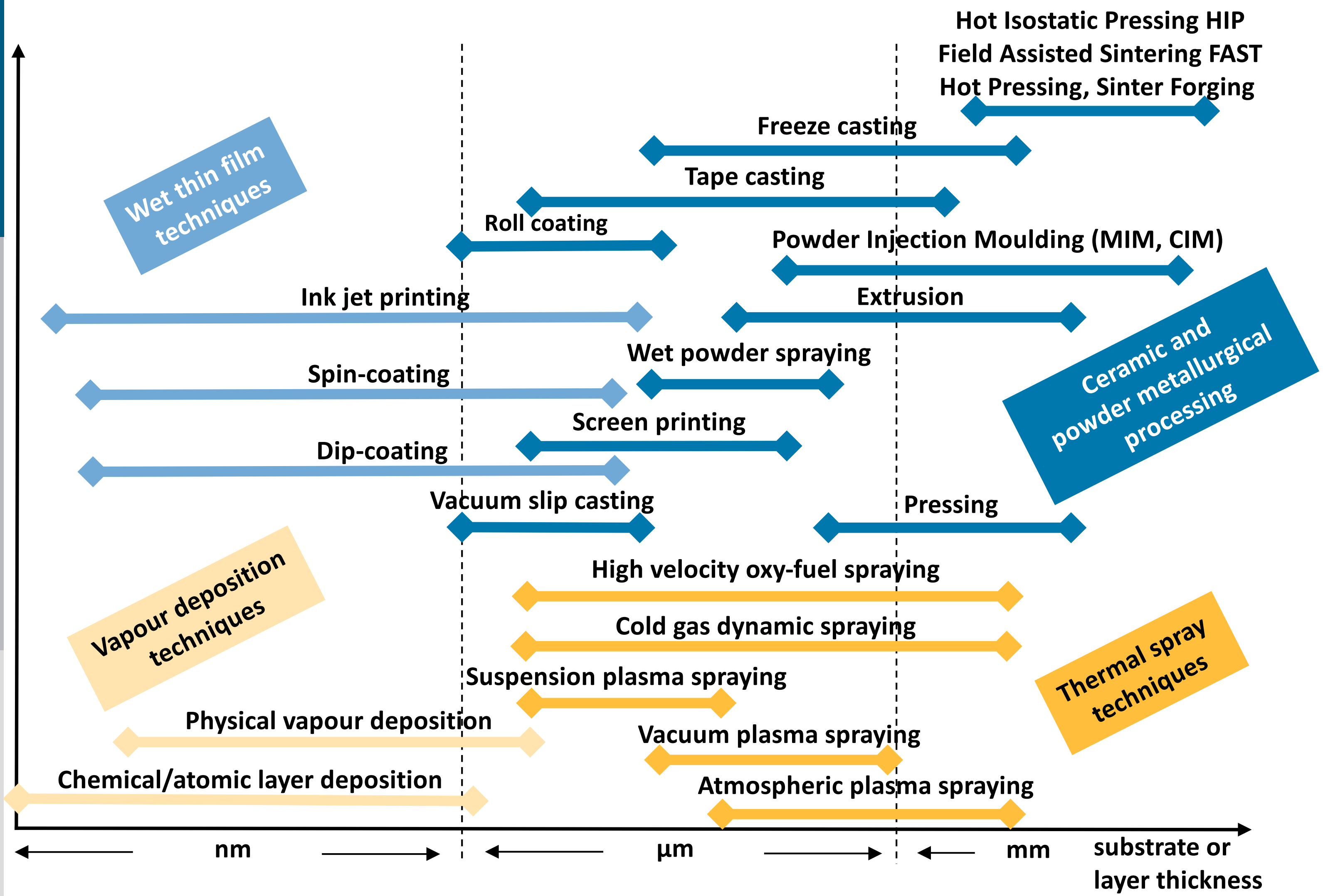

Large variety of processing methods in use for geometries from <1 µm up to 500 mm width and layer thicknesses down to sub-nanometre

Outline

Materials for
power plants

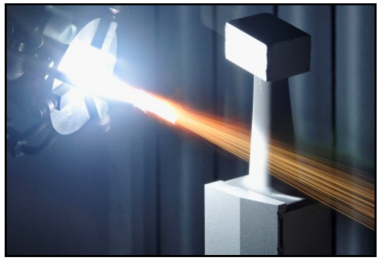

Gas separation membranes

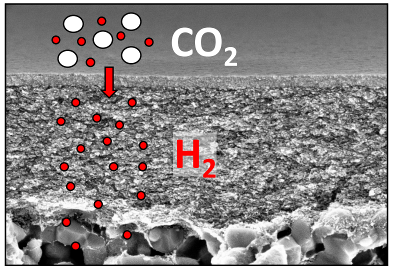

Solid oxide cells

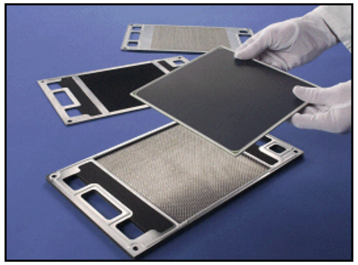

Electrochemical storage

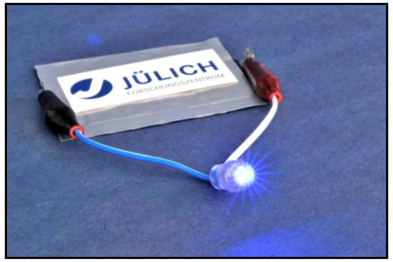

Development of ceramic membranes

Gas supply

Power Plants, Cement Industry (GREEN-CC), Glas Industry, Steel Industry, etc.

Membrane reactors

Chemical Industry (Syngas Production, Dehydration, Water-Gas-Shift-Reaction, etc.)

Material development

Stable Functional Materials in dependence of **thermal**, **chemical** and **mechanical** load

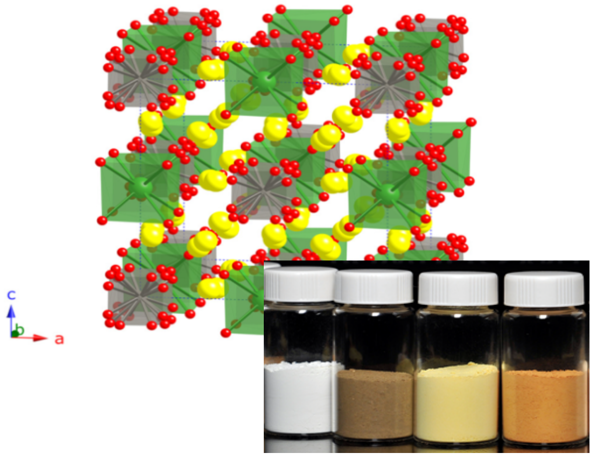

Microstructuring

Asymmetric Membranes with tailored microstructure for **flux optimisation.**
Application of catalysts

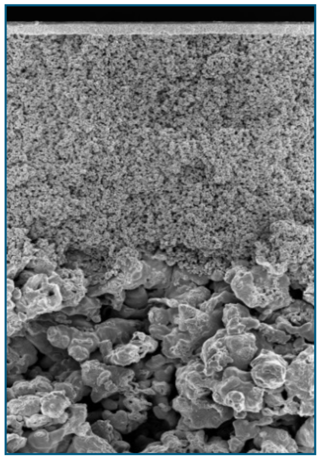

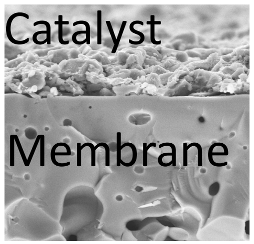

Component Manufacturing

Upscaling of **Membrane components** to application relevant scale for PoC-Modules

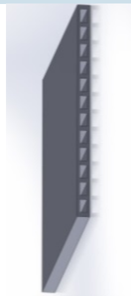

JÜLICH FORSCHUNGSZENTRUM

Gas Separation Membranes

Dense Membranes

Mixed Proton Conducting Membranes

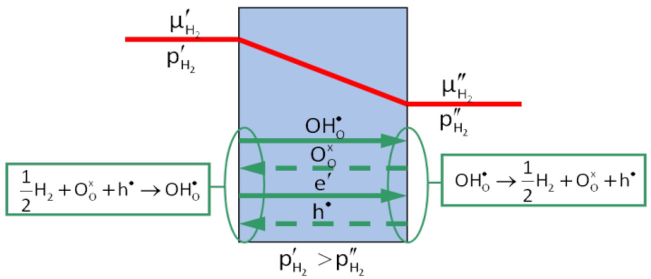

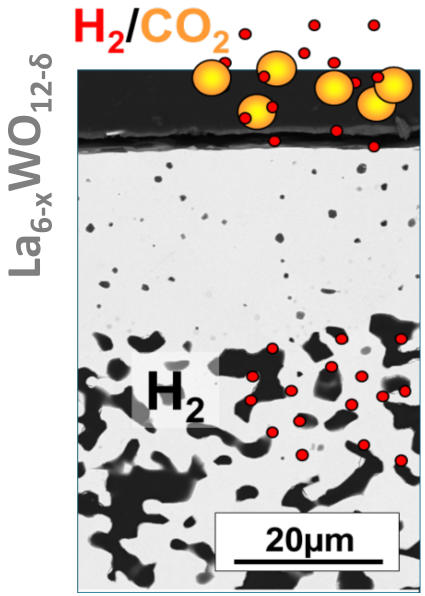

***T* = 600-800° C**

Mixed Oxygen Conducting Membranes

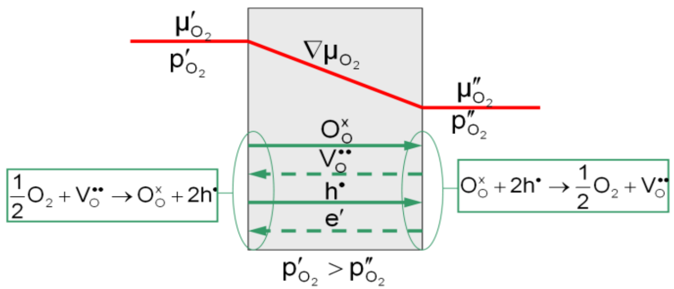

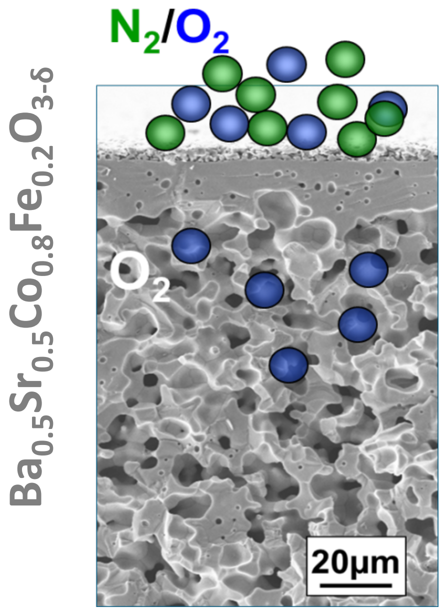

***T* = 800-900° C**

Microporous Membranes

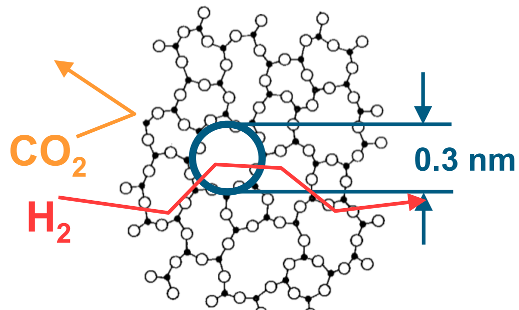

Amorphous network

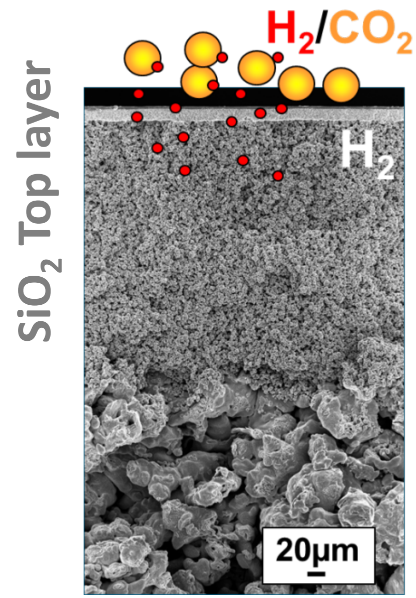

***T* ≈ 200° C**

Oxygen Transport in Mixed Conductors

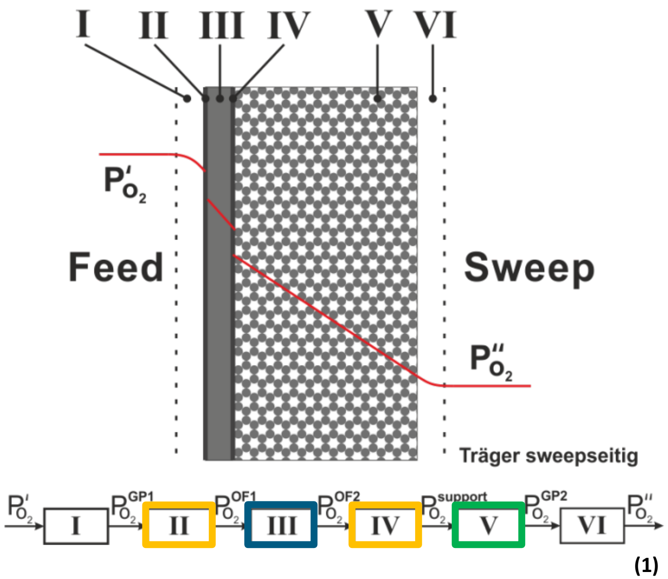

I & VI Gas transport

II & IV Surface Exchange

III Bulk Diffusion

V Gas transport in support

Zone III Bulk Diffusion

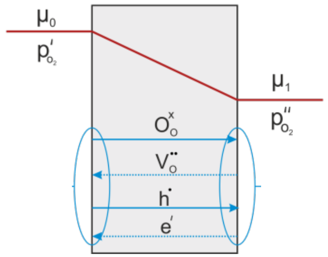

$$j_{O_2} = \frac{RT}{(4 \cdot F)^2} \cdot \frac{1}{L} \cdot \int_{\ln p'_{O_2}}^{\ln p''_{O_2}} \frac{\sigma_i \cdot \sigma_e}{\sigma_i + \sigma_e} \, d\ln p_{O_2}$$

Zone II & IV Surface Exchange / Kinetics

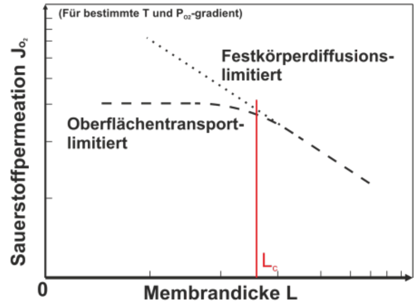

$$j_{O_2} = -\frac{1}{L + 2L_c} \cdot \frac{RT}{16 \cdot F^2} \cdot \frac{\sigma_i \cdot \sigma_e}{\sigma_i + \sigma_e} \cdot \ln \frac{p'_{O_2}}{p''_{O_2}} \quad (2)$$

$$L_c = \frac{D^*}{k}$$ **Characteristic Thickness**

Zone V Gas Transport in Support

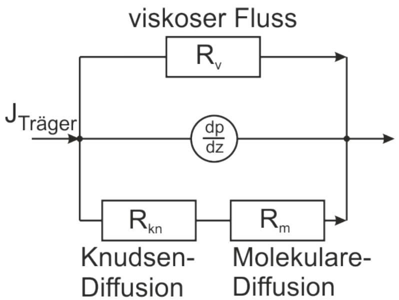

$$\underbrace{\nabla_{T,P} x_i + \frac{x_i}{p_{ges}} \nabla p_{ges}}_{\text{driving force}} = \underbrace{RT \sum_{j=1}^{n} \frac{(x_i \vec{j_j} - x_j \vec{j_i})}{P_{ges} D_{ij}}}_{\text{molecular diffusion}} \underbrace{- f_{im} \frac{RT}{p_{ges}} \vec{j_i}}_{\text{Knudsen-Diff. + viscous flow}}$$

(1) Schulze-Küppers, Diss. Ruhr-Universität Bochum (2010)

(2) Bouwmeester et al. Fundamentals of Inorganic Membrane Science and Technology (1996)

Membrane material selection (for H_2)

JÜLICH FORSCHUNGSZENTRUM

Material class	Perovskite-type	Defective fluorite-type
	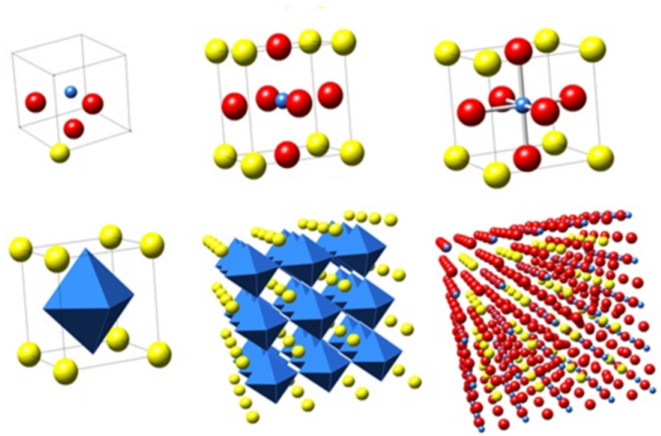	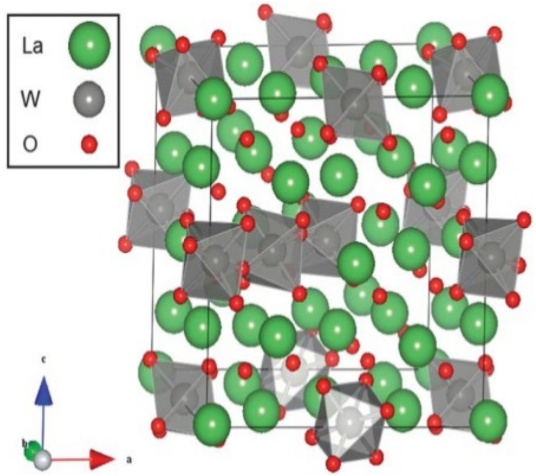
Material systems	$BaZrO_3$ and $BaCeO_3$	$La_{6-x}WO_{12-\delta}$
Properties	+ Large negative H_{hydr} + High stability of protons + Lowest E_{act} (σ_{prot}) + $\sigma_{prot.,b}$ ~10^{-2} S/cm + Ability to host cations - Limited stability - High intrinsic GB resistivity (e.g.: Y:$BaZrO_3$, Gd:$BaCeO_3$)	+ LaWO: $\sigma_{prot.}$ ~10^{-3} S/cm + Stable at HT, reducing atmospheres - Highest $\sigma_{prot.,b}$ at La/W=6 but 6:1 stoichiometry not stable - Narrow La/W phase stability range - Electronic conductivity must be improved

Materials with tailored conductivity

Macroscopic properties such as conductivity are controlled by microstructure

Example: Impedance plot of
$LaSrNbAlO_{4-\delta}$ at 400° C

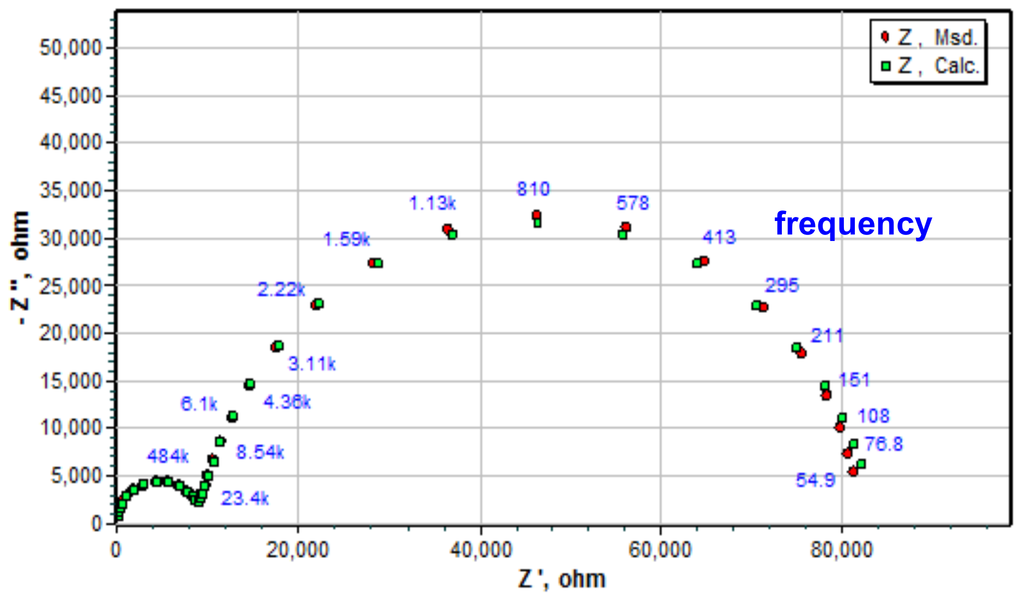

M. Ivanova et al., J Eur. Ceram. Soc. 35, 1239 (2015)

Equivalent circuit:

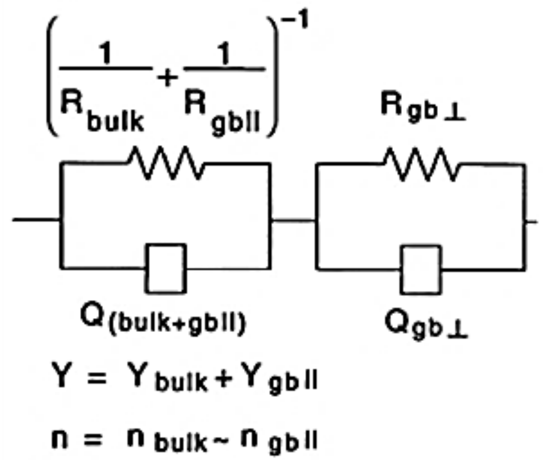

⇒ **Grain boundaries control the total conductivity**

Typology of grain boundaries

ELSEVIER

CrossMark

Available online at www.sciencedirect.com

ScienceDirect

Acta Materialia 62 (2014) 1–48

Acta MATERIALIA

www.elsevier.com/locate/actamat

Overview No. 152

Grain boundary complexions

Patrick R. Cantwell [a], Ming Tang [b,1], Shen J. Dillon [c], Jian Luo [d], Gregory S. Rohrer [e], Martin P. Harmer [a,*]

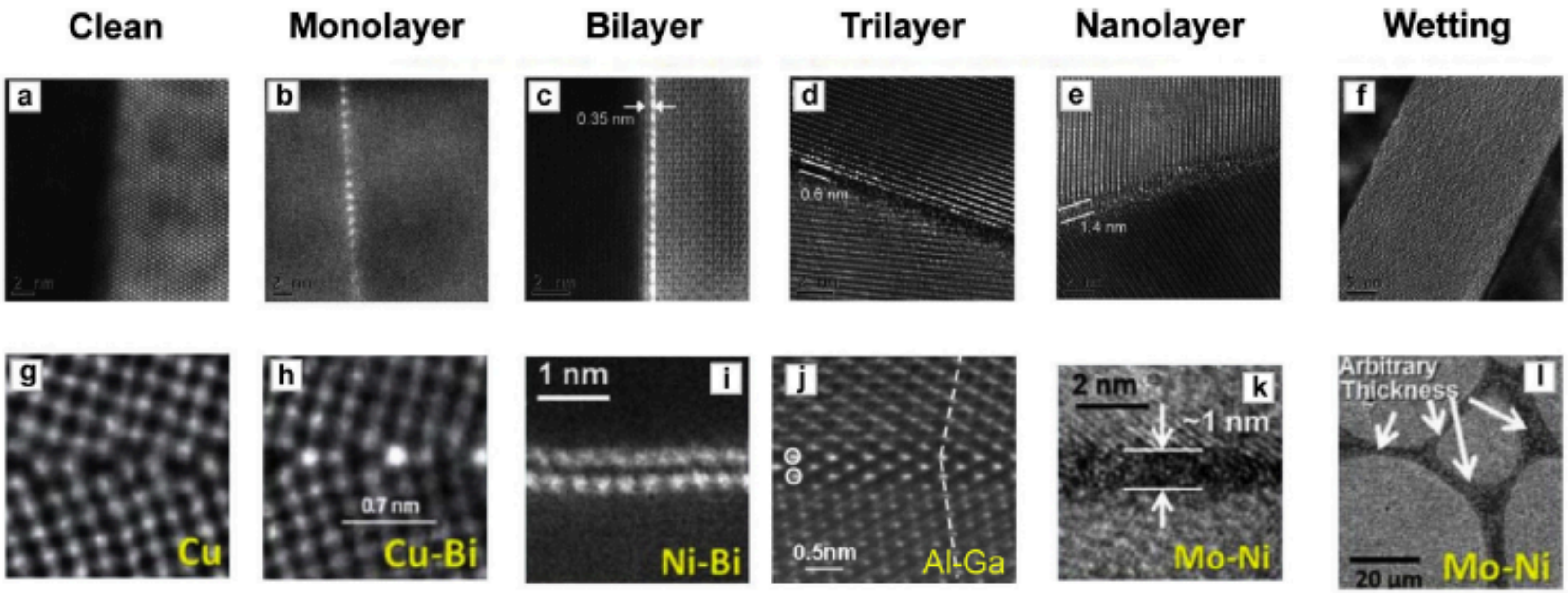

Grain boundary engineering

Contents lists available at ScienceDirect

Acta Materialia

journal homepage: www.elsevier.com/locate/actamat

Full length article

Expanding time–temperature-transformation (TTT) diagrams to interfaces: A new approach for grain boundary engineering

Patrick R. Cantwell [a], Shuailei Ma [b], Stephanie A. Bojarski [c], Gregory S. Rohrer [c], Martin P. Harmer [b, *]

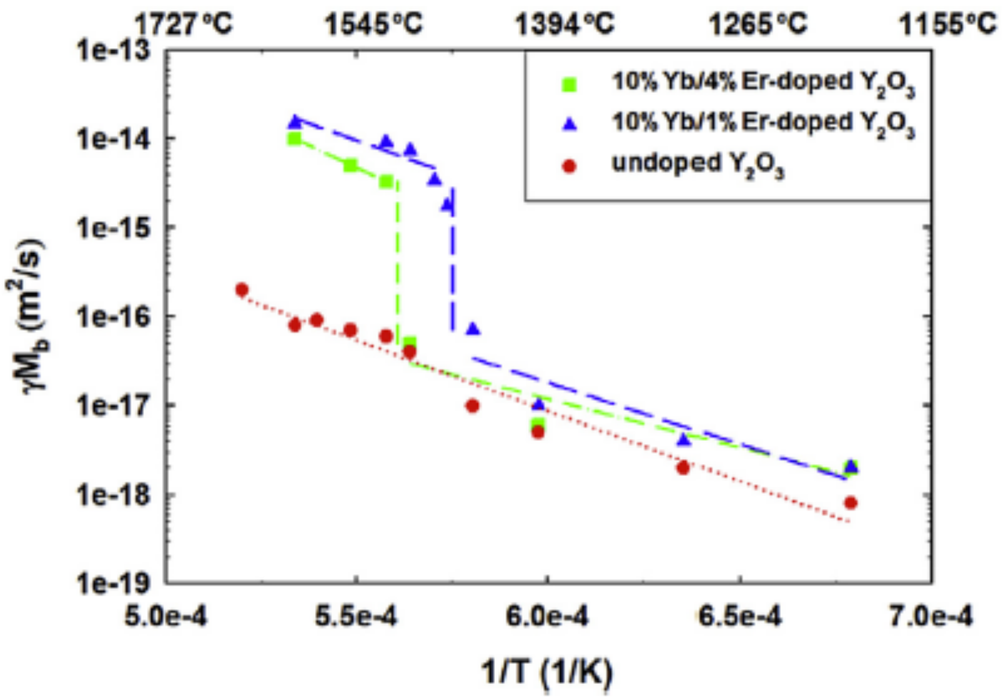

Dual-phase membrane for H_2-separation

$BaCe_{1-x}Eu_xO_{3-\delta}$: $Ce_{1-y}(Y,Eu)_yO_{2-\delta}$

- Perovskite phase with proton conductivity
- Fluorite phase with electronic conductivity and stabilization role against perovskite decomposition under CO_2 atmosphere

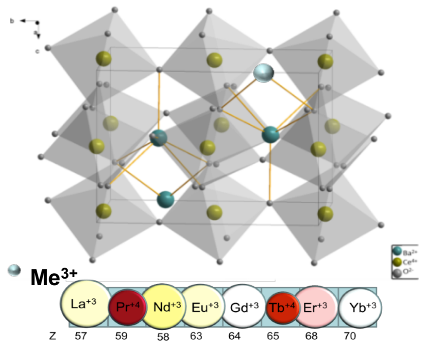

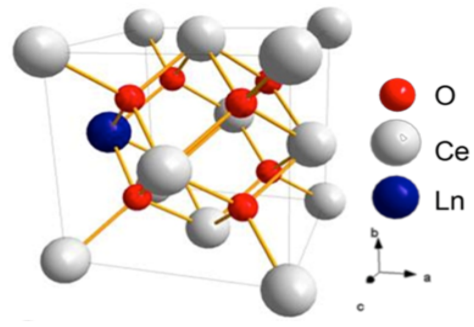

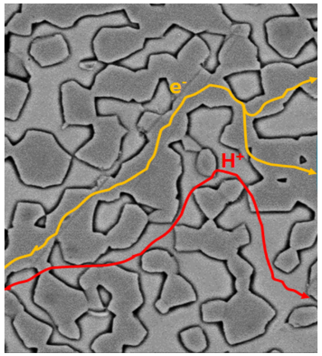

- High percolation degree of the two phases
- Two ceramic phases chemically and thermally compatible
- Unprecedented H_2-flux at 700° C, high catalytic activity for water splitting

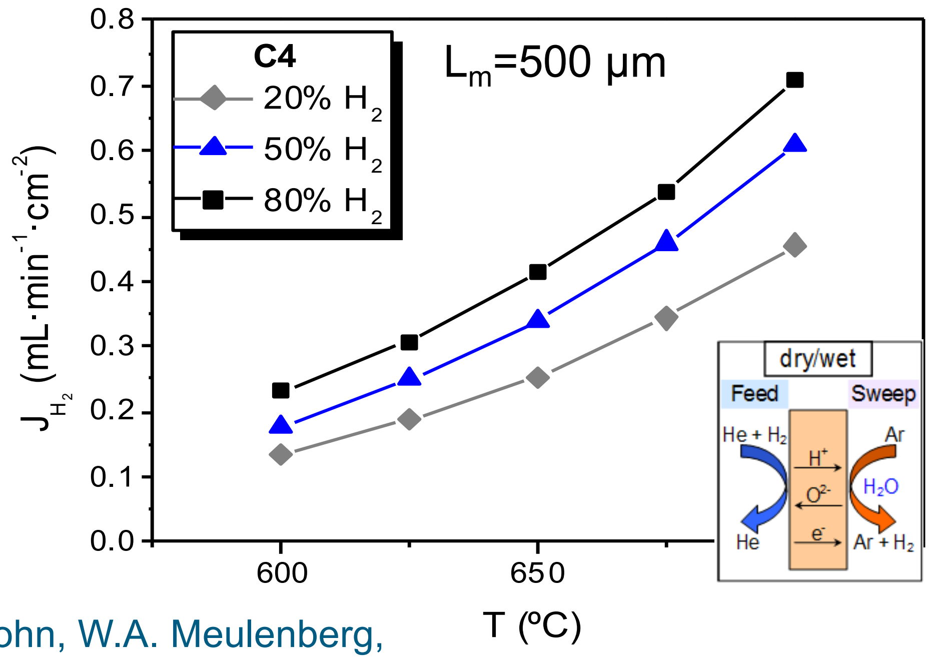

M.E. Ivanova, S. Escolastico, M. Balaguer, J. Palisaitis, Y.J. Sohn, W.A. Meulenberg, O. Guillon, J. Mayer, J.M Serra, Scientific Reports, 2016

Stability and Materials Compatibility

JÜLICH FORSCHUNGSZENTRUM

Catalytic Membrane reactor (4-End-Mode)

Feed stream: Synthesis gas $CO + H_2O$ ($+H_2$) →

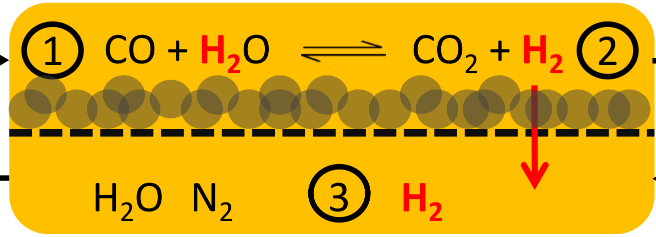

→ Retentate (**CO_2**, H_2O)

← Permeate: Fuel (**H_2, N_2**, H_2O)

← Sweep gas (**N_2**, H_2O)

gas compositions

	content /vol.-%		
component	1	2	3
H_2	15	0.1	34
CO_2	-	**90**	-
CO	**34**	-	-
H_2O	51	9.9	2.5
N_2	-	-	**63**

materials

membranes	catalysts
high H_2-flux	catalytic activity
high selectivity of H_2	high selectivity
thermochemical and microstructural stability	
compatibility of membrane and catalyst	

Exposure conditions T = 600 -900 ° C **Δ T** = 100 ° C, **p_{atm}**, **t** = 72h

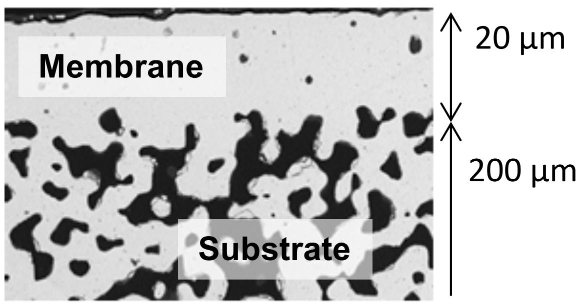

D. van Holt, *et al.*, J. Eur. Cer. Soc. 34, 2381–2389 (2014)

Catalyst, Ø 1 – 2 mm
Example: Fe_2O_3/Cr_2O_3

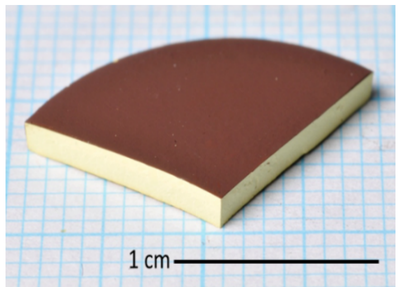

Screen printed *cat layer* on a membrane

Development of membrane components

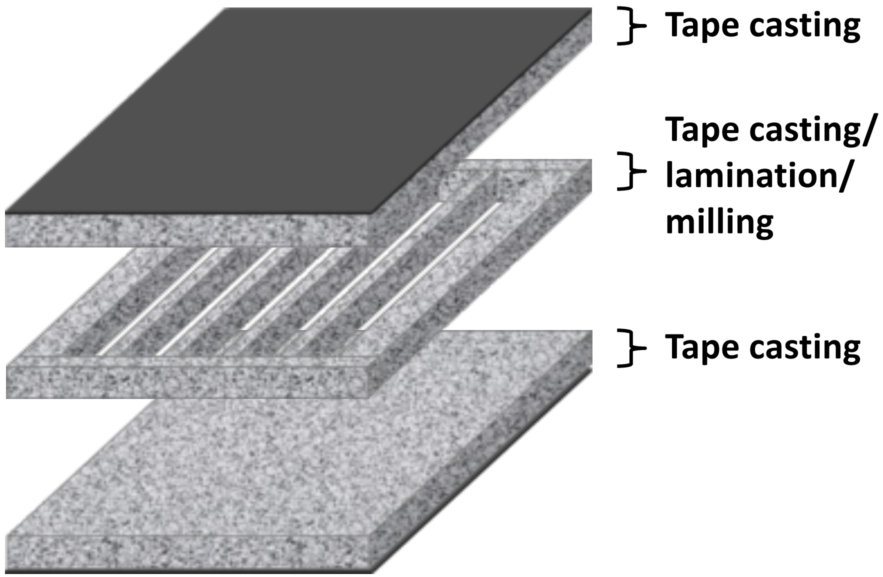

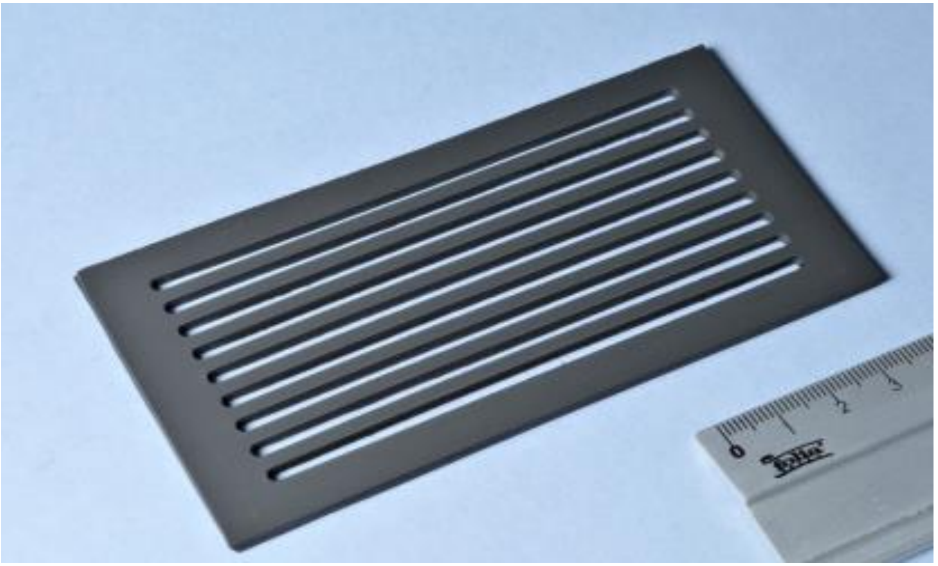

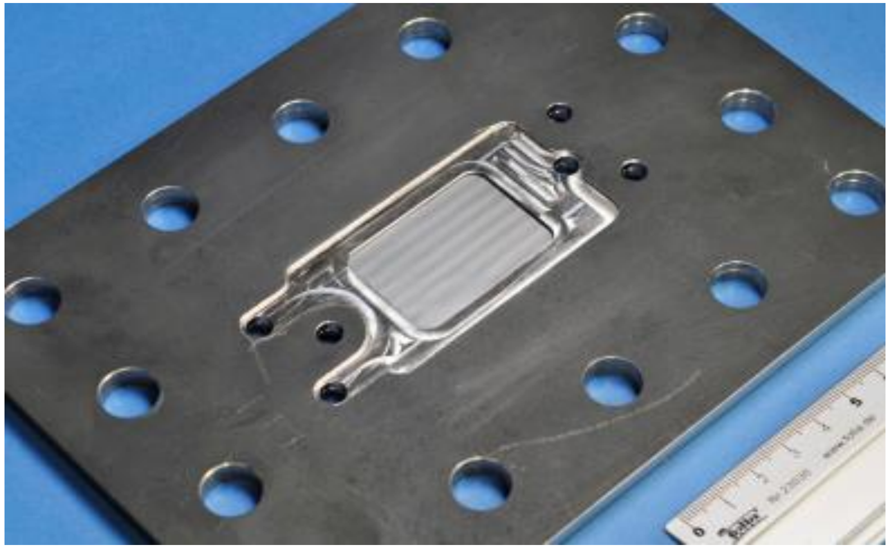

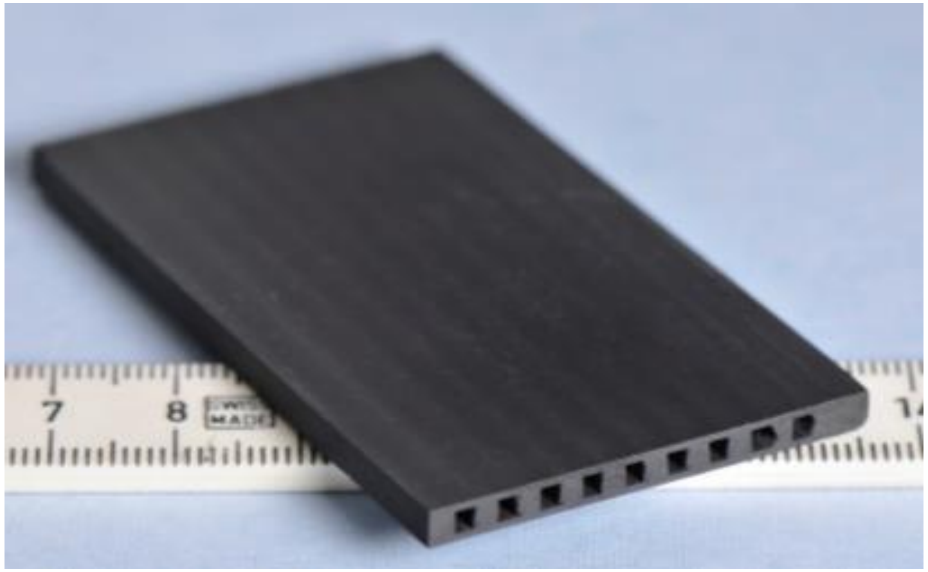

F. Schulze-Küppers, S. Baumann, W. Meulenberg et al.

Outline

Materials for power plants

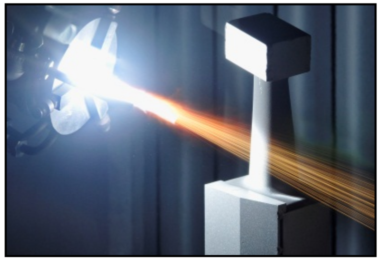

Gas separation membranes

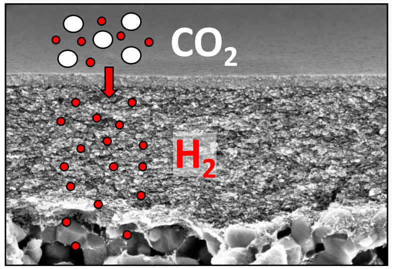

Solid oxide cells

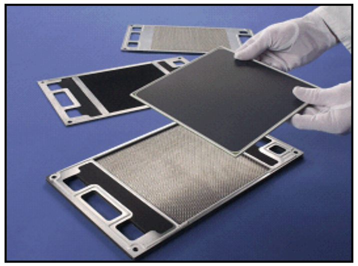

Electrochemical storage

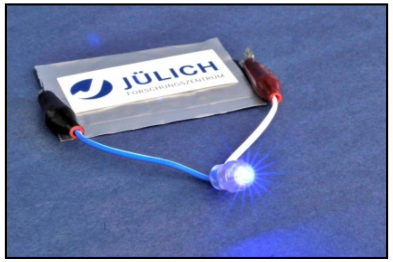

Solid oxide cells

JÜLICH FORSCHUNGSZENTRUM

Anode-supported cells

SOFC
„Fuel-to-Power“

SOEC
„Power-to-Fuel“

ROB
„Power-to-Storage“

Decentralized energy supply

Intermediate storage of volatile electricity / Fuel production

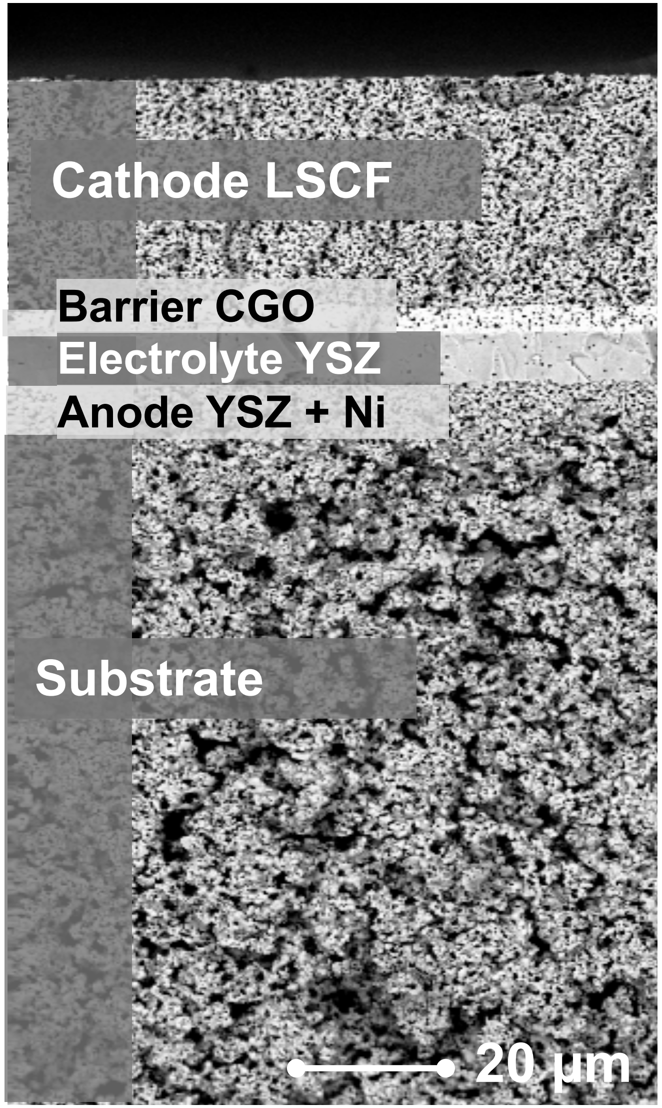

Metal-supported cells

Christian Doppler Forschungsgesellschaft

PLANSEE

AVL

Auxiliary Power Units

JÜLICH
FORSCHUNGSZENTRUM

IEK-2 Microstructure and Properties
Steel, thermomechanics, thermochemistry

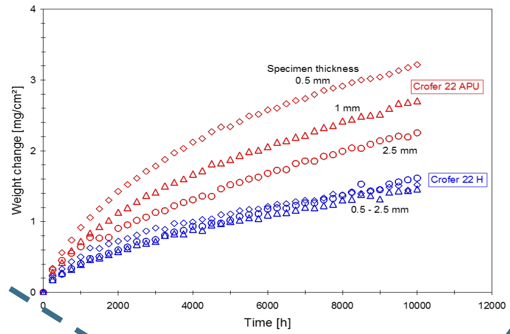

IEK-3
Electrochemical Process Engineering
Stack test, system development & modelling

IEK-1
Materials Synthesis and Processing
Cell development, contacting

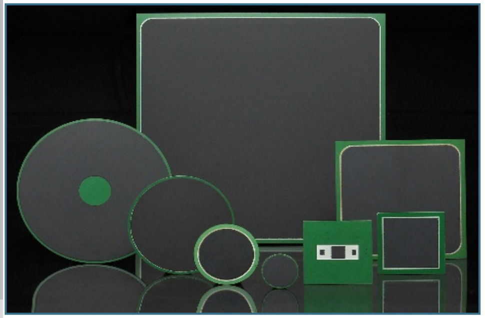

Jülich SOFC development

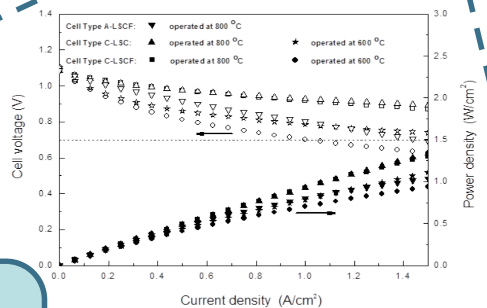

ZEA-1
Central Institute for Engineering
Sealing, welding, stacking

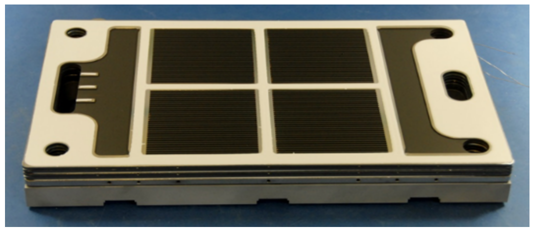

IEK-9
Fundamentals of Electrochemistry
Cell testing and analysis

SOFC/SOEC stack

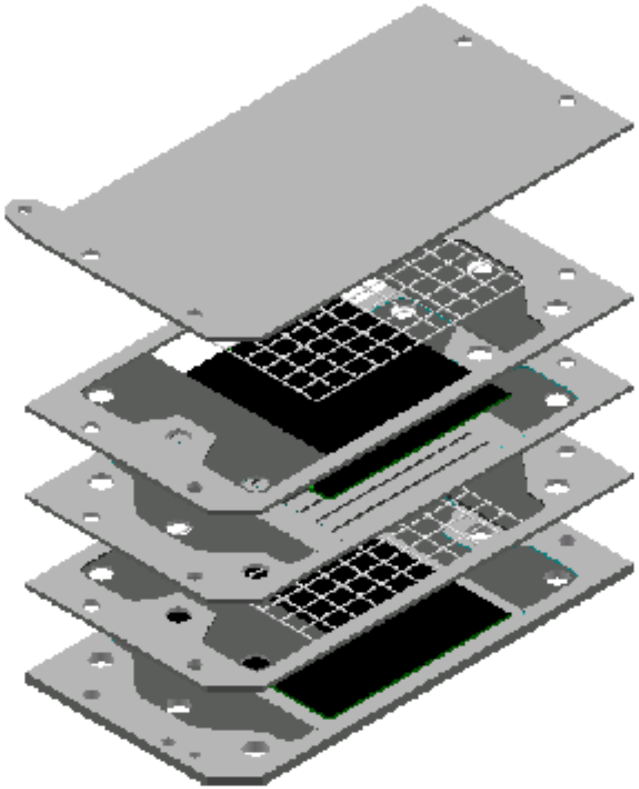

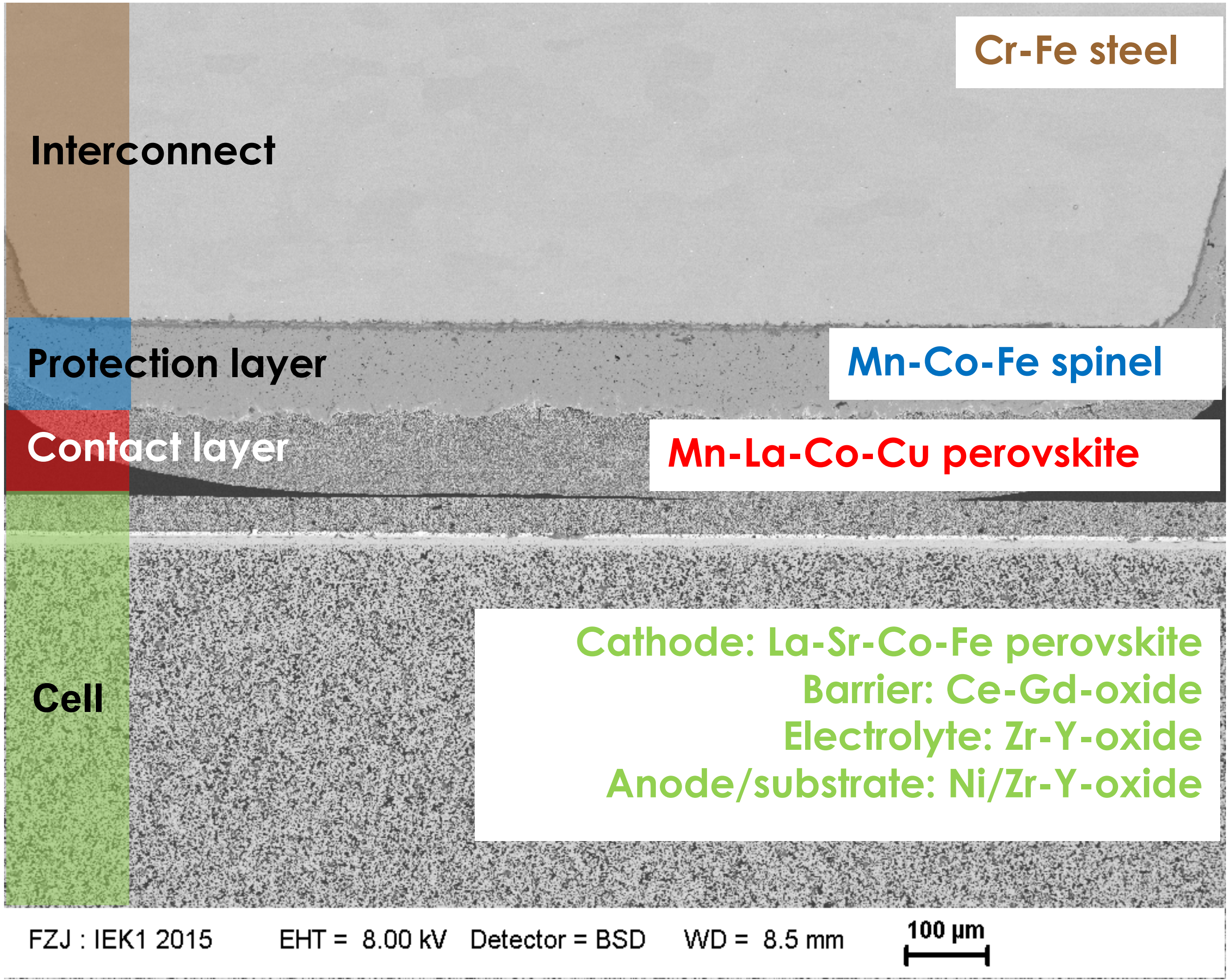

Long-term stack operation

Operating time under load

66,600 h @ 0.70 %/kh
34,500 h @ 0.30 %/kh

Degradation rate

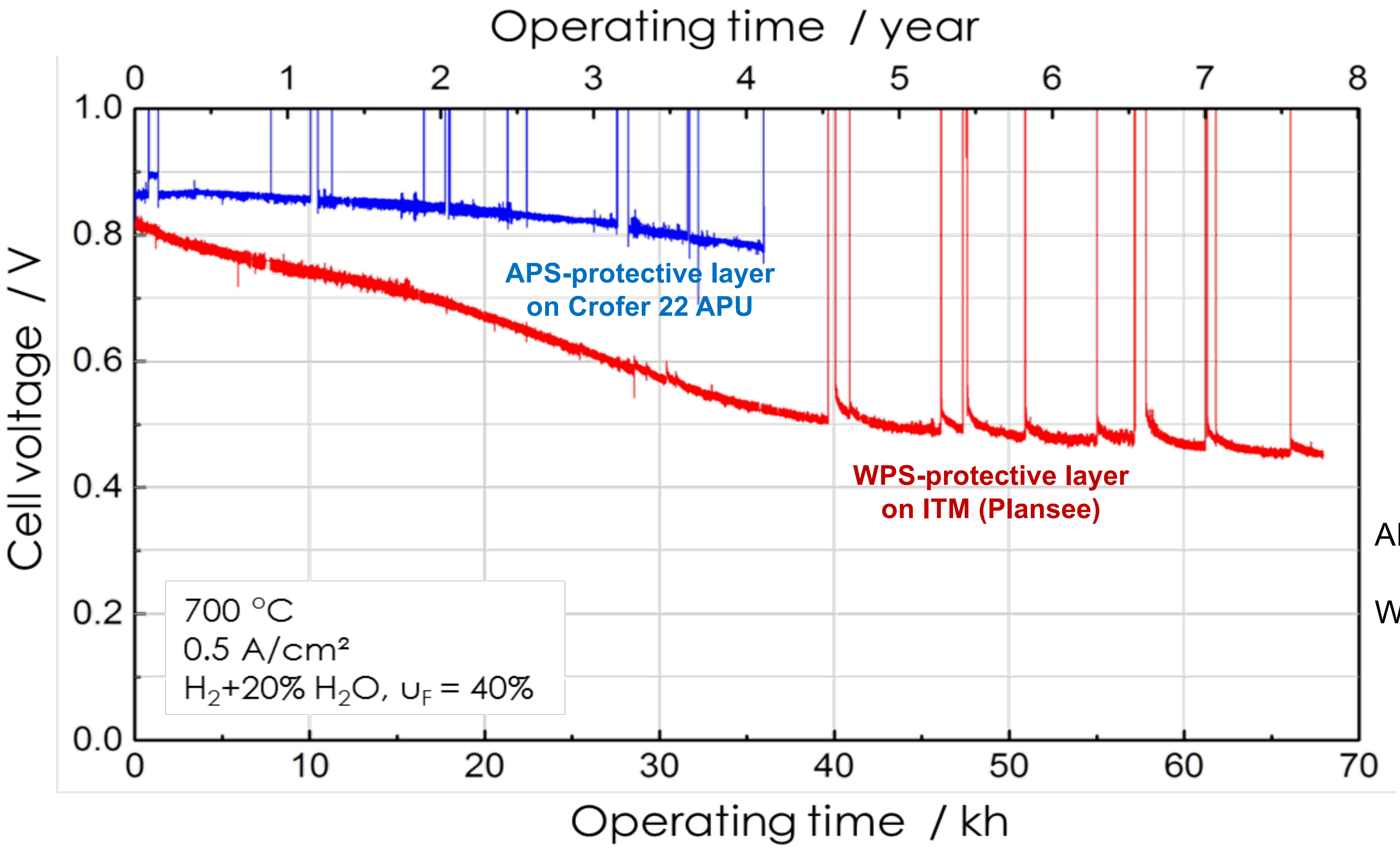

Short Stacks
$10x10\ cm^2$
2 resp. 4 layers

APS – atmospheric plasma spraying
WPS – wet powder spraying

SOFC - Degradation

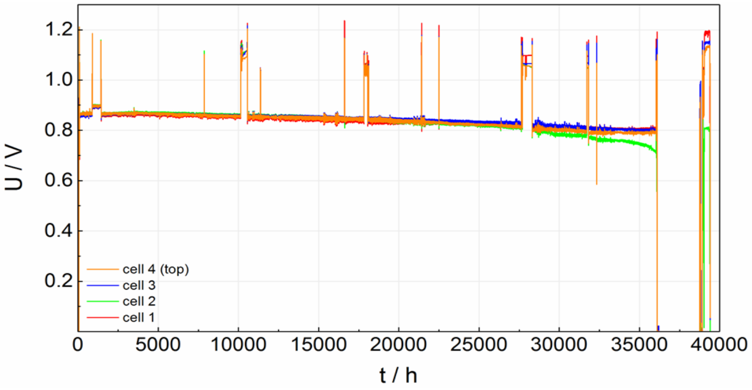

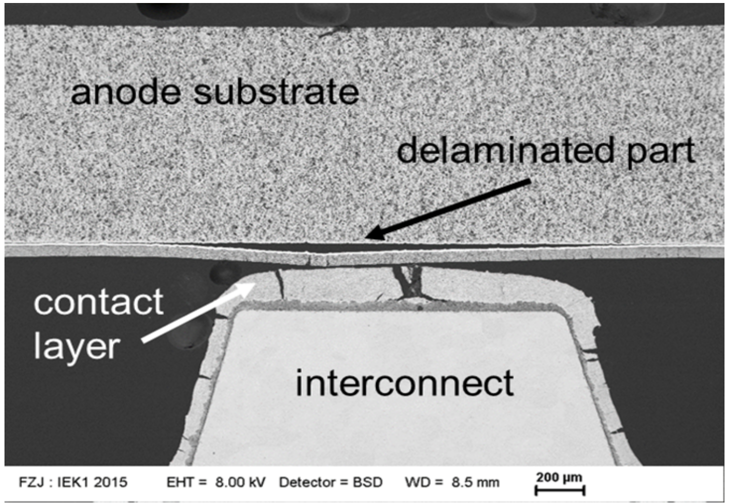

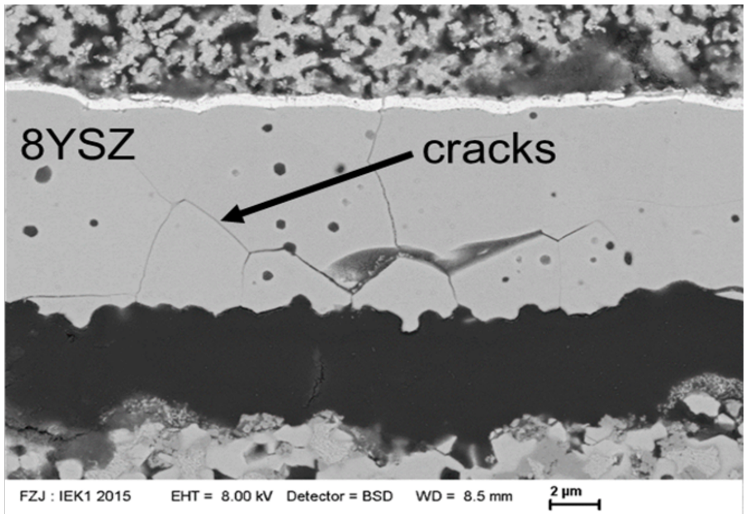

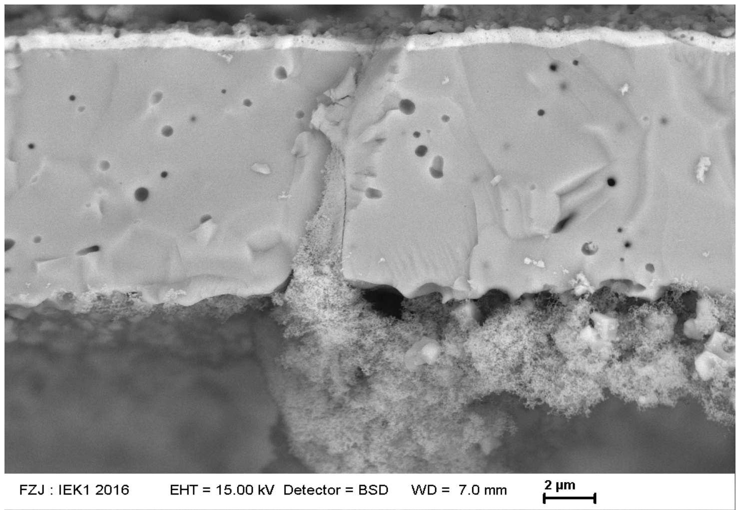

Crack and secondary phase formation in electrolyte and at electrolyte/anode interface.

Hypothesis:
Mn diffusion via solid state diffusion through gas tight barrier and electrolyte.

Under reducing conditions (fuel side!) sponge-like secondary phase formation.

Menzler N.H., Batfalsky P., Beez A., Blum L., Groß-Barsnick S.-M., Niewolak L., Quadakkers W.J., Vaßen R.
Proc. 12th Europ. SOFC & SOE Forum, 05.-08.07.2016, Lucerne, CHE

Rechargeable oxide batteries

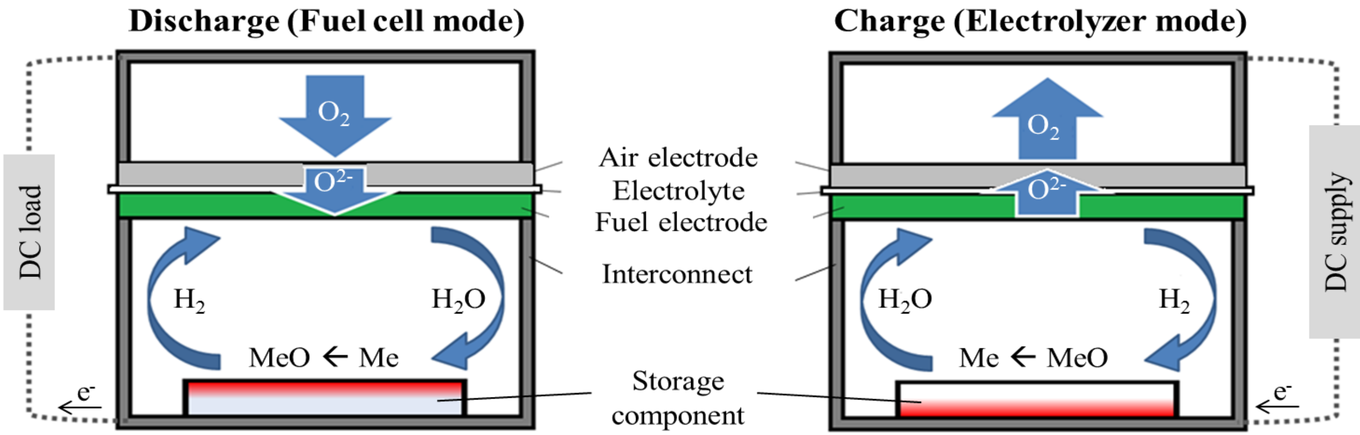

Development of storage material: e.g. FeO/YSZ mixture or mixed oxide(s) of FeO and CaO

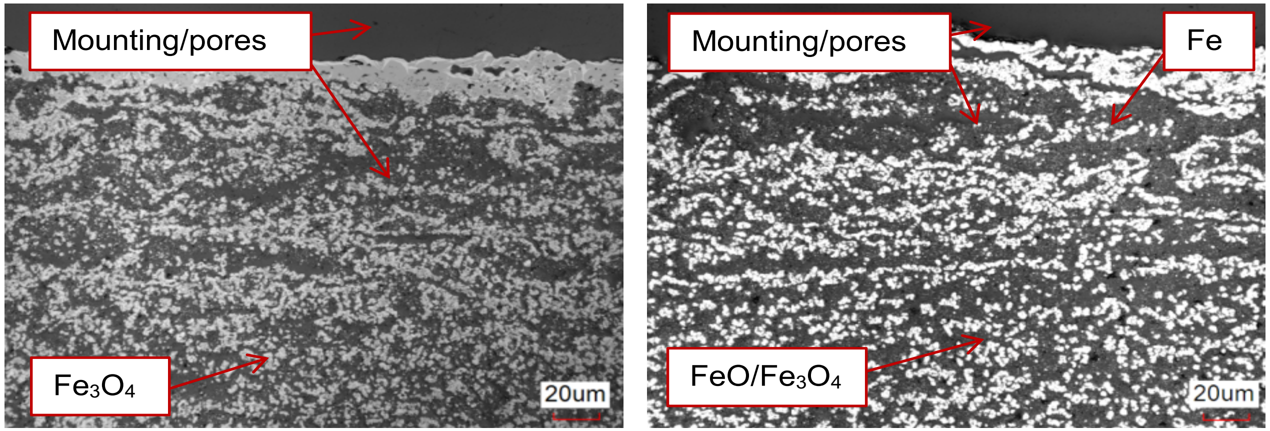

FeO/YSZ storage after 10 (left, oxidized) or 11 (right, reduced) half cycles; slight agglomeration and rim formation visible

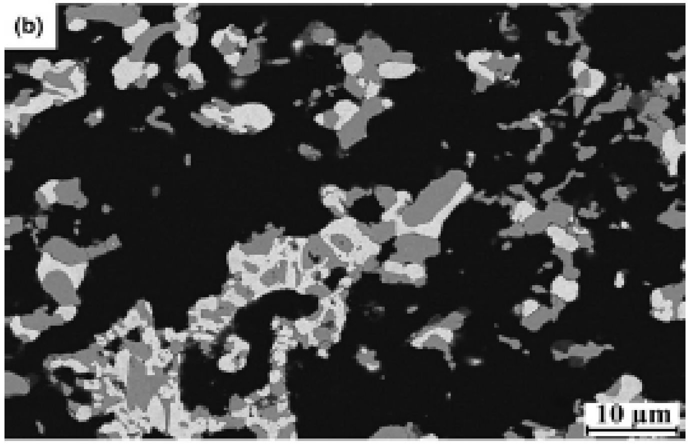

$Ca_xFe_yO_z$ storage after 11 redox cycles; microstructure remains stable

Berger C.M. et al. J. American Ceramic Society 99 [12] (2016), 4083-4092
Berger C.M. et al. J. Energy Storage 1 (2015), 54-64

Outline

Materials for power plants

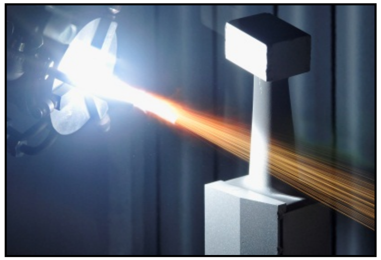

Gas separation membranes

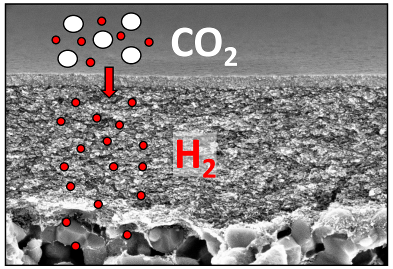

Solid oxide cells

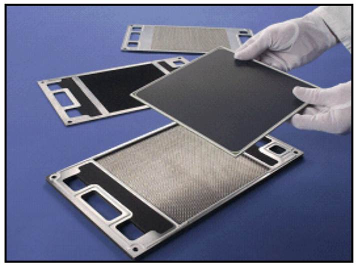

Electrochemical storage

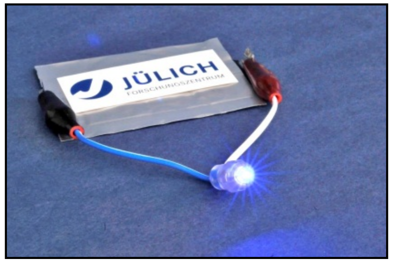

Solid-State Batteries

Safety
- No leakage
- No combustion
- Less toxic
- Less reaction with air and moisture

Stability
- Use of “high voltage” materials
- Use of metallic Li/Na (high capacity)

  ⇒ higher energy density
- Temperature stability

Higher integration
- Better packaging, no balancing required
- Easier thermal management

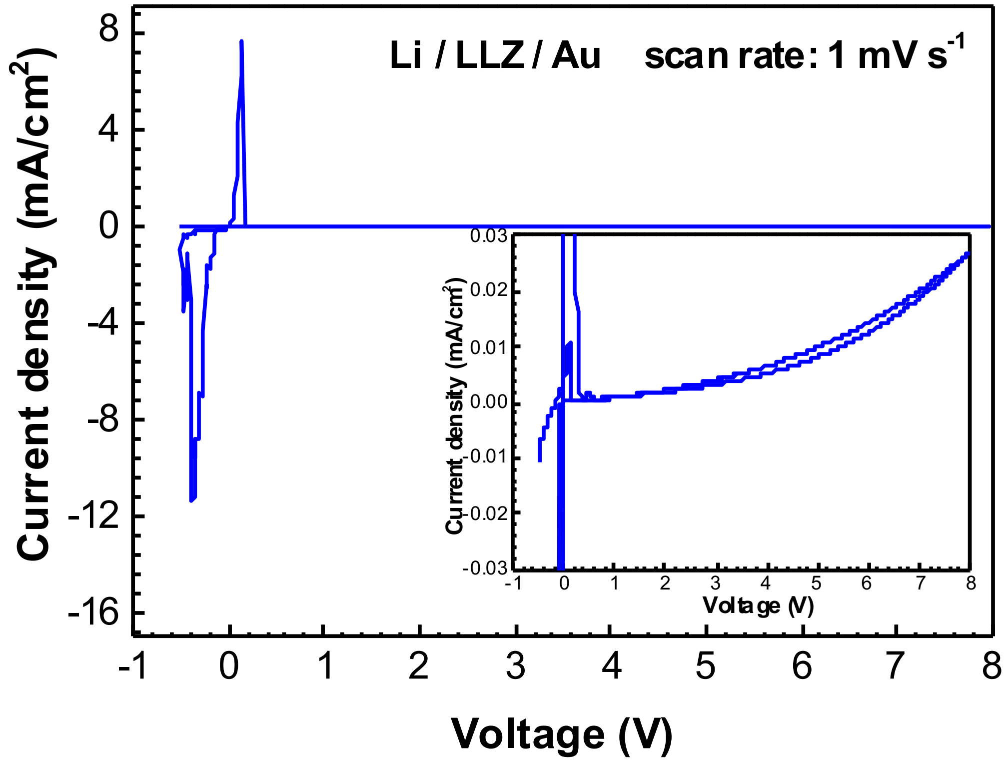

- Lower conductivity of solid electrolytes compared to liquid electrolytes
- Contact resistance at the interfaces

Solid-State Electrolytes

Requirements:

- High Li^+ ionic conductivity ~10^{-3} S/cm at room temperature
- Negligible electronic conductivity < 10^{-9} S/cm
- Low grain boundary resistances (ceramics)
- Chemical stability against electrodes, especially metallic anode
- Wide electrochemical stability window
- Environmentally acceptable and non toxic
- Non-hygroscopic, stable in ambient atmosphere
- Low-cost raw materials, simple processing

→ **No solid-state electrolyte fulfills all criteria!**

Battery research at IEK-1

Cathode development for high-voltage Li/Na-ion batteries

Electrolyte development for **Li/Na-batteries**

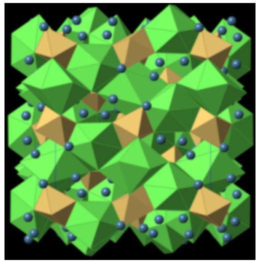

$Li_7La_3Zr_2O_{12}$

Materials development

Ceramic processing

Thin film technologies

All-solid-state batteries

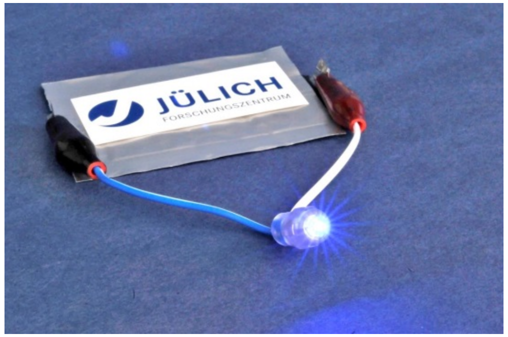

$LiCoO_2$ / $Li_7La_3Zr_2O_{12}$ / Lithium-Metal

Processing of self supporting electrolytes and mixed cathodes

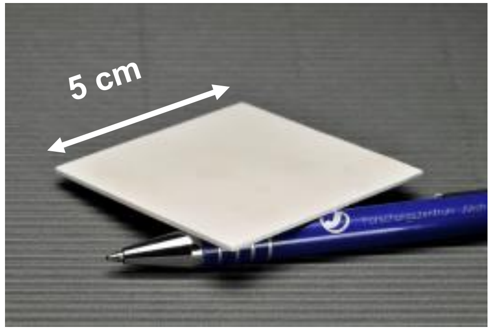

Manufacturing of all-solid-state batteries

Minimization of interface resistances

Maximal use of theoretical capacity

Deposition of thin inorganic layers

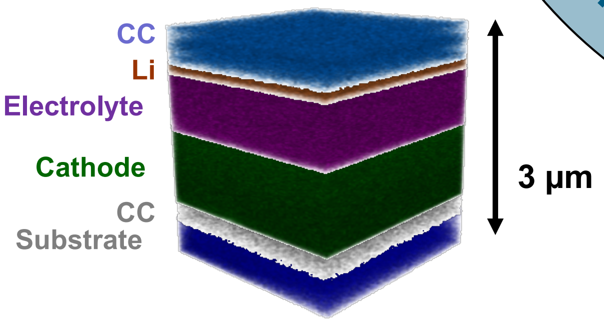

Comparison between Na and Li-ion batteries

Characteristics	Na	Li
Price (for carbonates)	0.07 - 0.37 € kg^{-1} (Purity 98.8 – 99.2 % min)	4.11 – 4.49 € kg^{-1} (Battery grade 99.9 %)
Specific capacity	1.16 A h g^{-1}	3.86 A h g^{-1}
Voltage vs. S.H.E.	- 2.7 V	- 3.0 V
Ionic radius	0.98 Å	0.69 Å
Melting Point	97.7 °C	180.5 °C

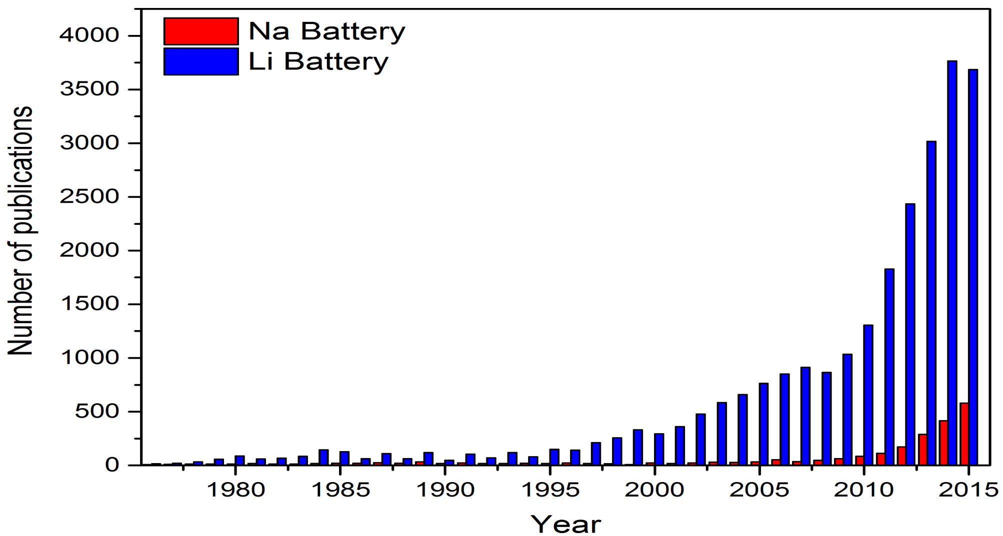

Electrolytes currently under investigation

NASICON-type material

- $Li_{1+x}Al_xTi_{2-x}(PO_4)_3$
- $Na_{1+x+y}Sc_xZr_{2-x}P_{3-y}Si_yO_{12}$

Garnet-type materials

- $La_3Zr_2Li_{7-3x}Al_xO_{12}$ (LLZ:Al)
- $La_3Zr_{2-x}Ta_xLi_{7-x}O_{12}$ (LLZ:Ta)

Glass

- LiPON (thin films only)

Spray drying

LLZ:Al (kg / batch)

Novel sol-gel method (LATP):

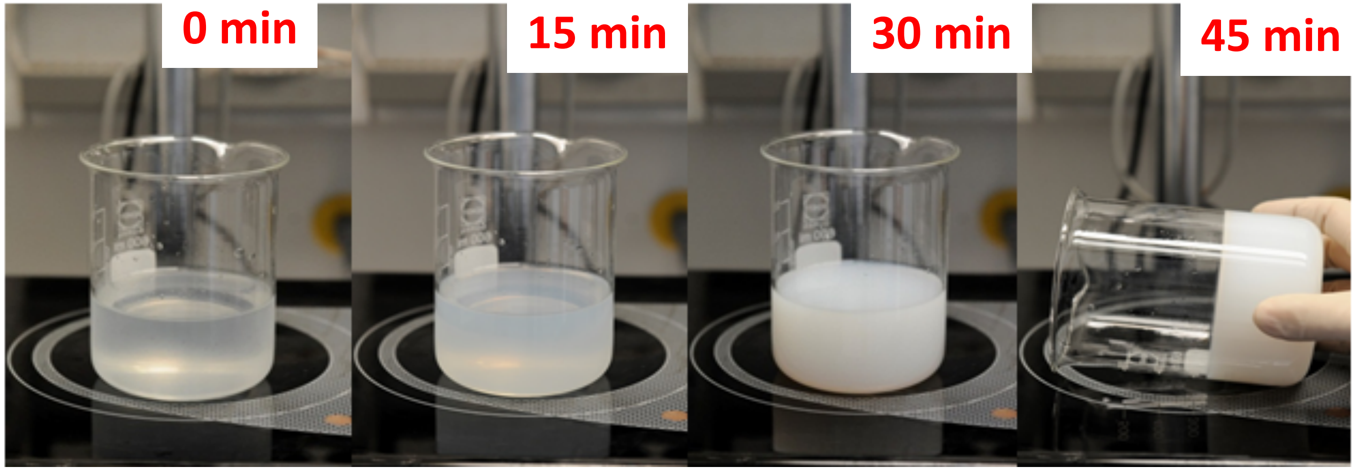

✓ Cheap chemicals, simple lab equipment, easy processes
✓ Easy scaling-up of production (kg / batch)
✓ Good powder qualities (easy sintering, phase purity, high conductivity)

Q. Ma, F. Tietz , O. Guillon, Patent DE 10 2014 012 926, 2014;
Q. Ma et al. Journal of the American Ceramic Society, 2016

Processing of solid electrolytes

JÜLICH FORSCHUNGSZENTRUM

1 mm

100 µm

10 µm

1 µm

100 nm

10 nm

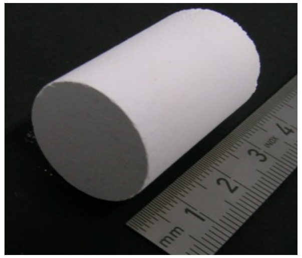

Pressing; for materials properties characterization

5 orders of magnitude

Tape casting

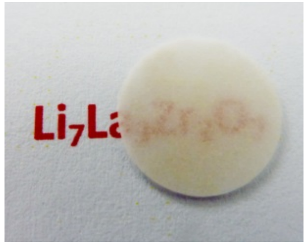

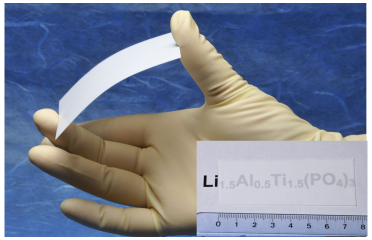

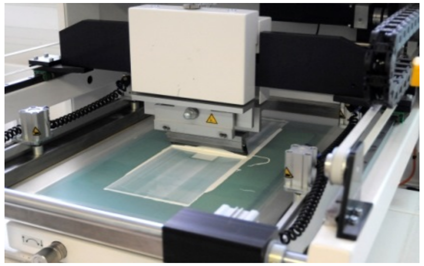

Screen-printing

Powders sintered to high density

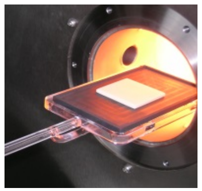

Physical Vapor Deposition

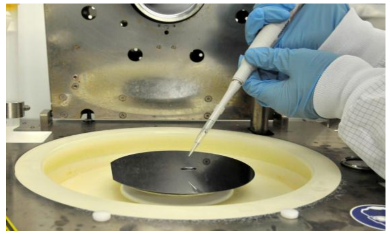

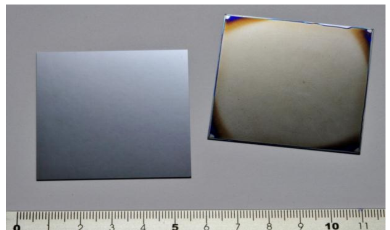

Sol-Gel, Micro-emulsion

Na^+ conducting electrolytes: NASICON

(**Na S**uper **I**onic **CON**ductors)

$$\left([A]^{+a} \; [MM']^{+m} \; [(PO_4)_3]^{-9} \right)^{+a+m-9=0}$$

A	••alkali cations , alkaline earth cations, H^+, H_3O^+, NH^{4+}, Cu^+, Cu^{2+}, Ag^+, Pb^{2+},Cd^{2+}, Mn^{2+}, Co^{2+}, Ni^{2+}, Zn^{2+}, Al^{3+}, Ln^{3+} (rare earth), Ge^{4+}, Zr^{4+}, Hf^{4+} and it can also be vacant
MM′	••di-, tri-, tetra-, pentavalent cations
$(PO_4)_3$	••P can be partially substituted by Si or As

Hong, H.Y.-P. Materials Research Bulletin, 1976. 11: p. 173-182.
Hong, H.Y.-P., J.B. Goodenough, and J.A. Kafalas. Materials Research Bulletin, 1976. 11: p. 203-220.

Understanding of transport properties in solid state sodium electrolytes

- Compositional optimisation necessary with respect to component manufacturing
- Easier processing is highly recommended as an alternative to ß-aluminas

M. Guin, F. Tietz,
Journal of Power Sources
2015

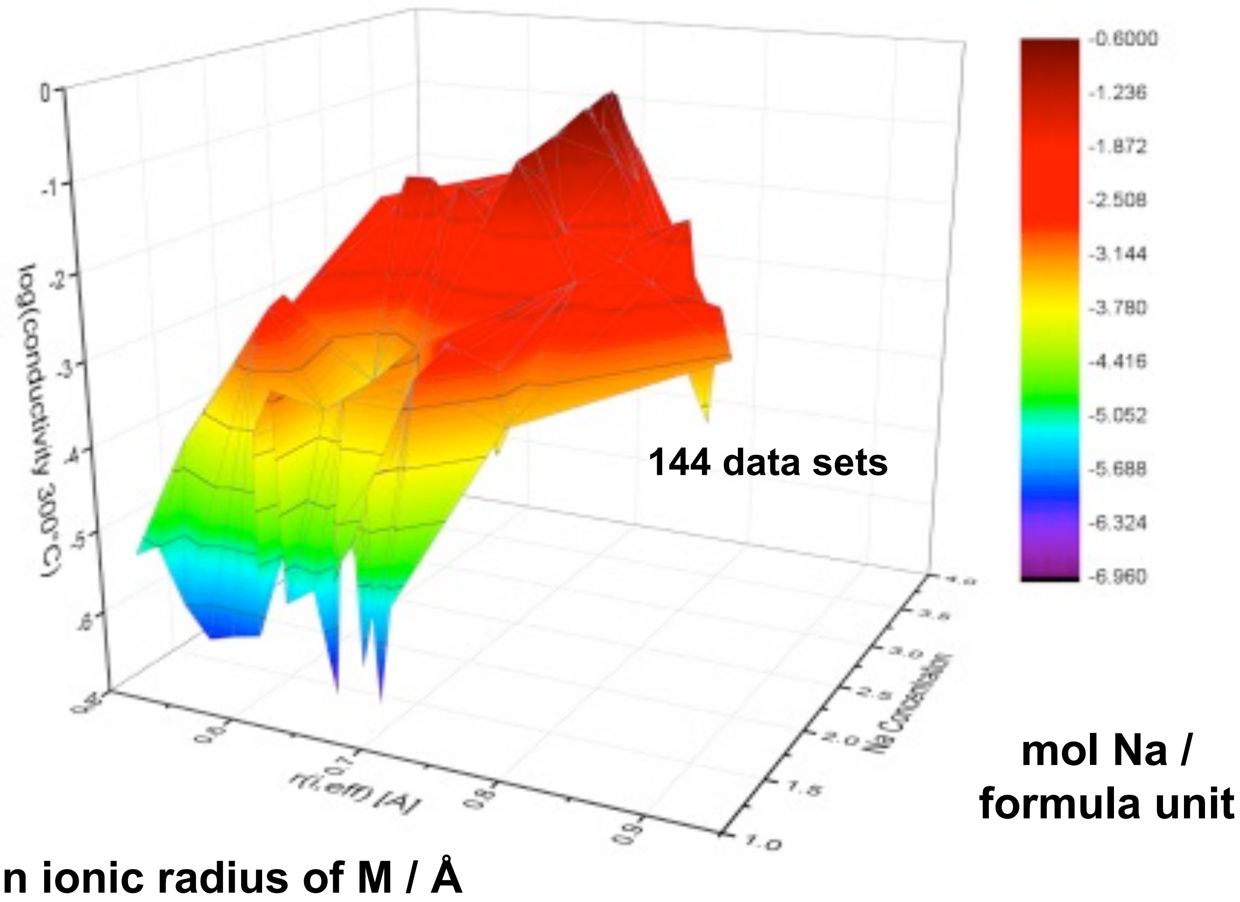

Design of a taylored electrolyte: $Na_{3+x}Sc_xZr_{2-x}(SiO_4)_2(PO_4)$

- Monoclinic crystal structure

– stabilization by Si

- Substitution of Zr^{4+} by Sc^{3+}:

– close ionic radii, in the optimal range

– increase of Na content

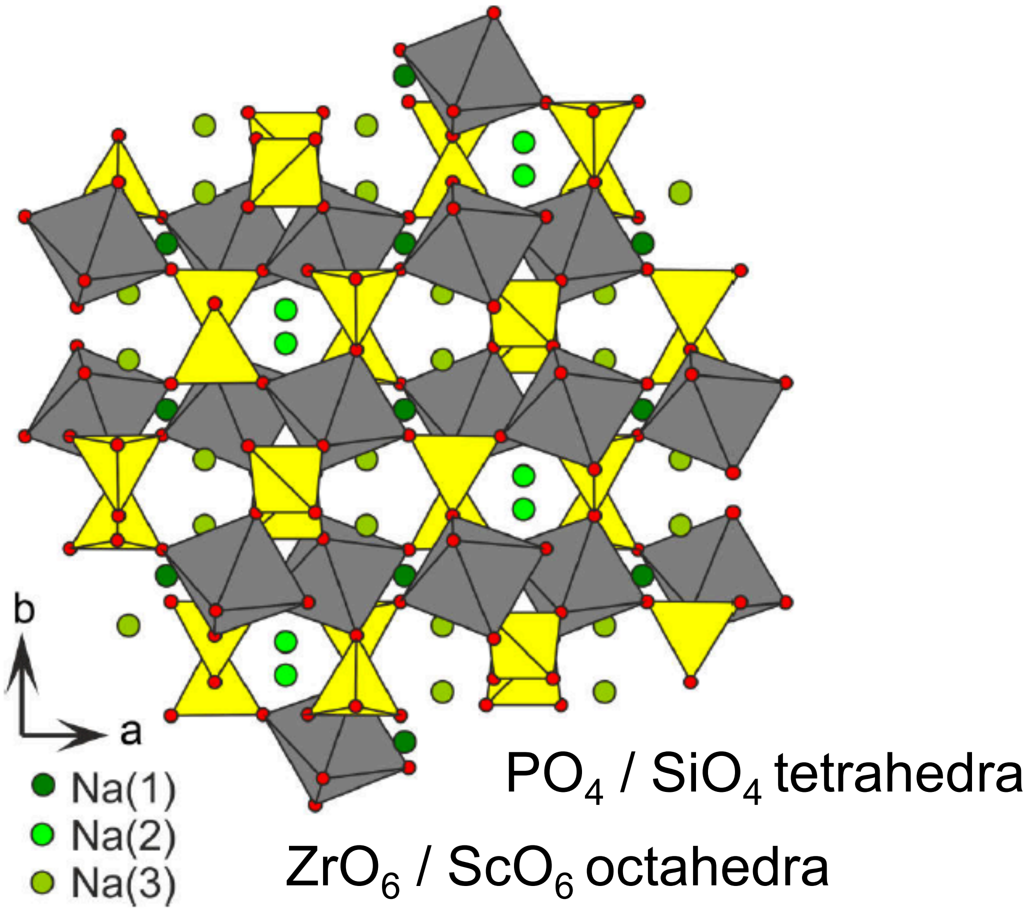

Conduction mechanism in $Na_{3+x}Sc_xZr_{2-x}(SiO_4)_2(PO_4)$

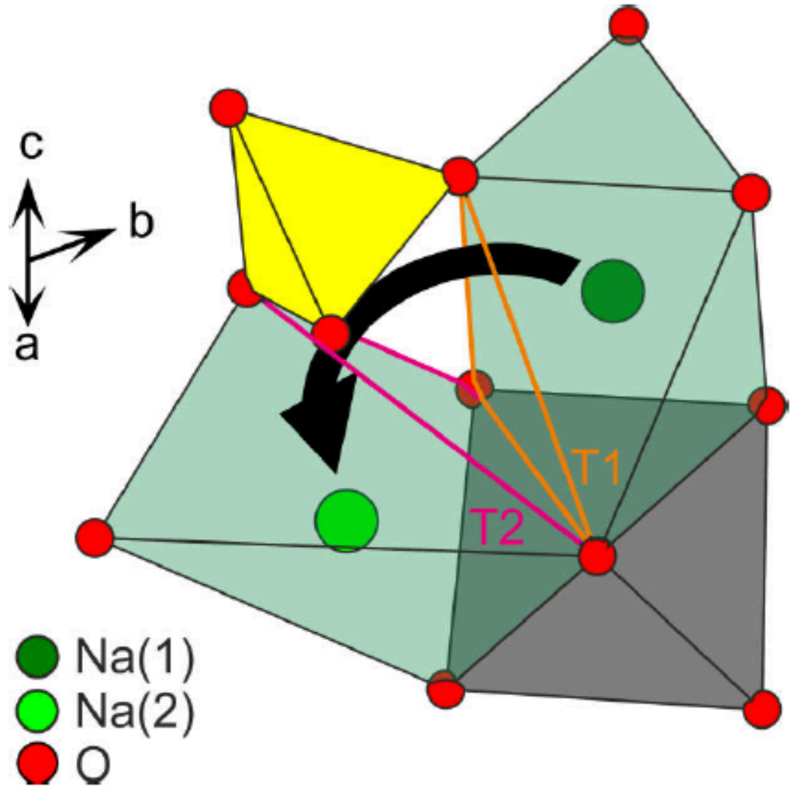

Possible relevant crystal lattice parameters:

- Distance between sodium positions
- Bottleneck size (triangle area)
- Distance between sodium and next oxygen

Correlation between lattice and conductivity

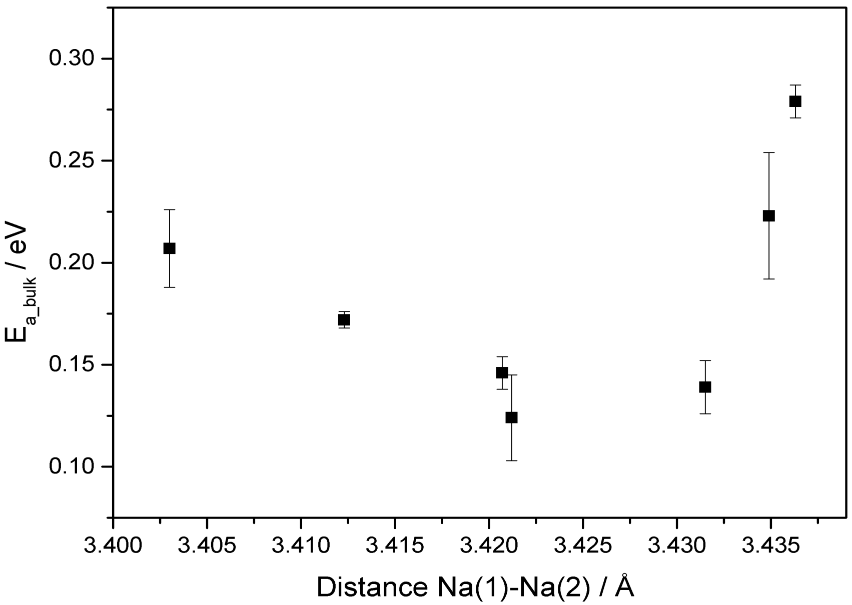

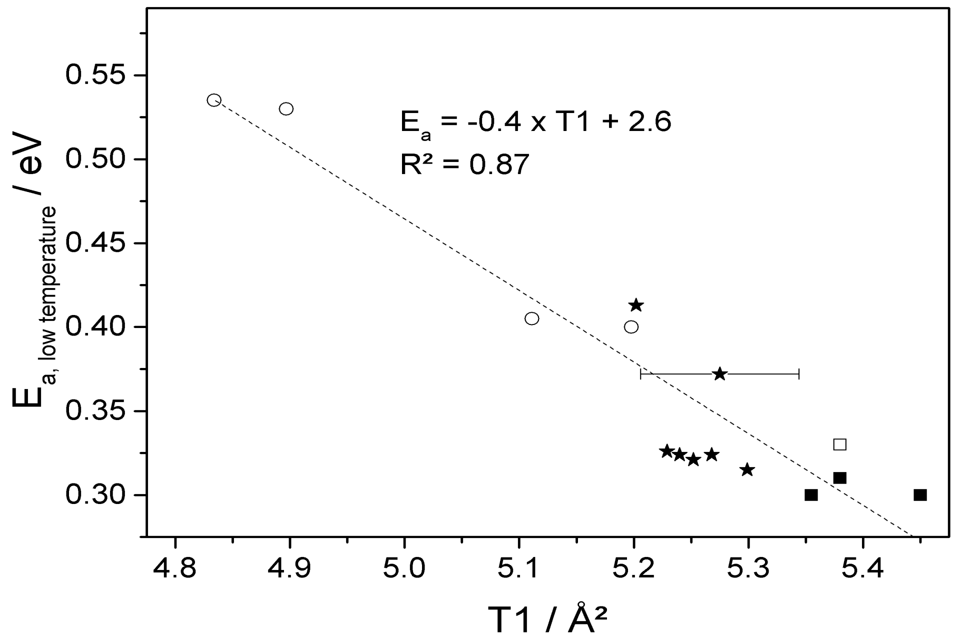

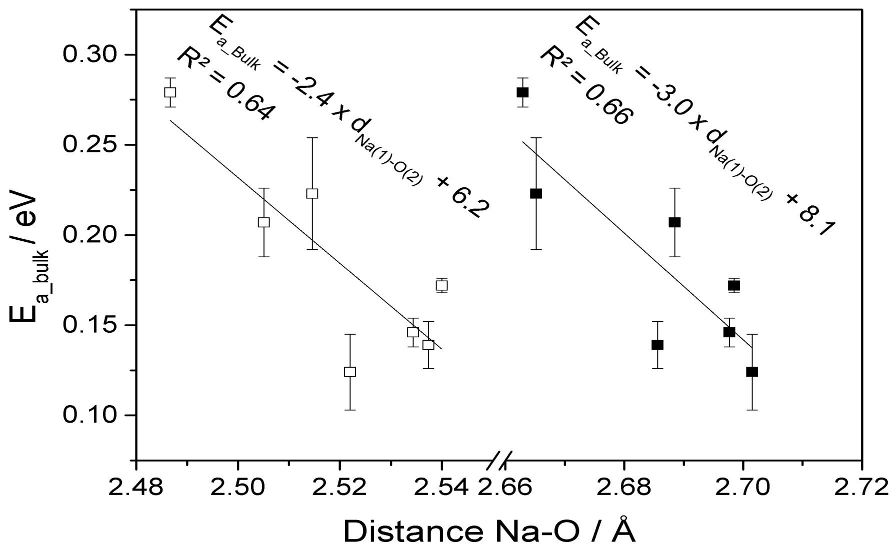

M. Guin, F. Tietz, O. Guillon, Solid State Ionics, 2016

Development of $Na_{3+x}Sc_xZr_{2-x}(SiO_4)_2(PO_4)$

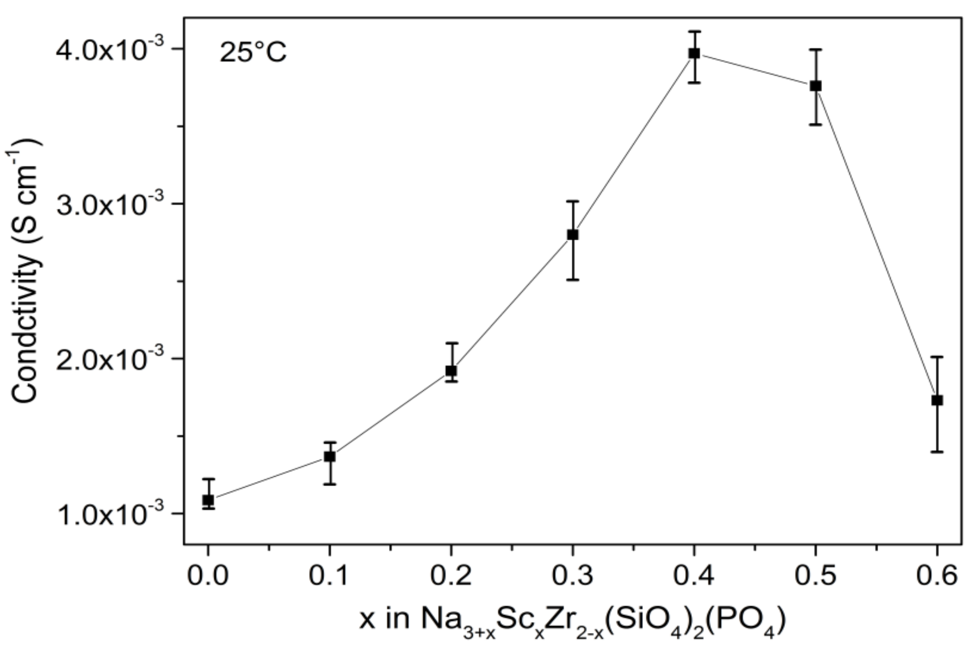

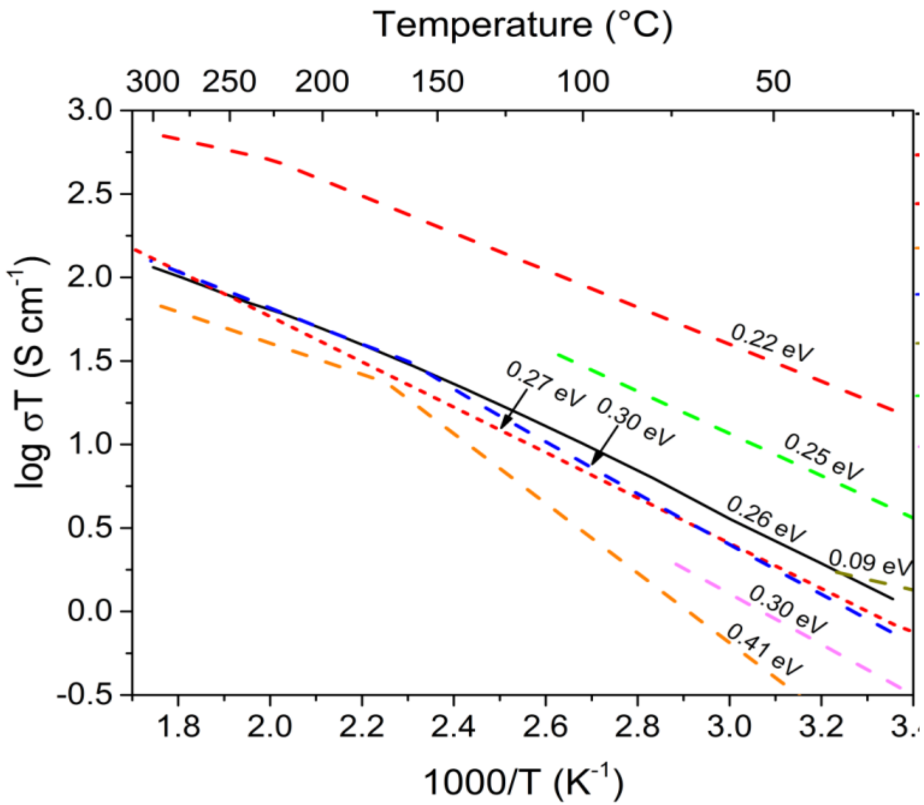

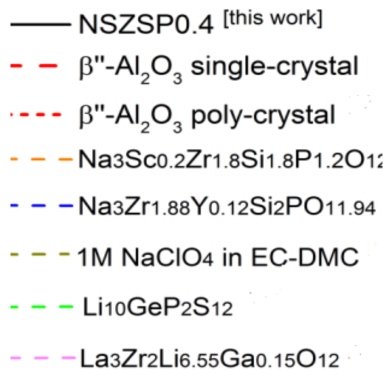

- NSZSP0.4 shows the highest conductivity (4 mS/cm) of all reported polycrystalline Na-ion conductors
- NSZSPx are electro-chemically stable up to 6 V vs. Na/Na^+ and show no reaction with Na metal.

Q. Ma, M. Guin, S. Naqash, C.-L. Tsai, F. Tietz, O. Guillon, Chem. Mater. 2016 (28) 4821

Physical Vapor Deposition of LLZ:Ta

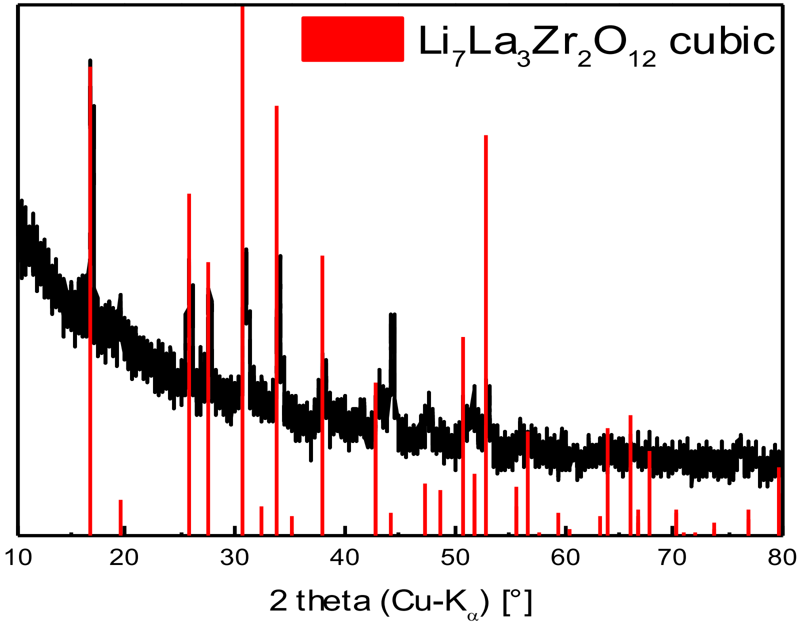

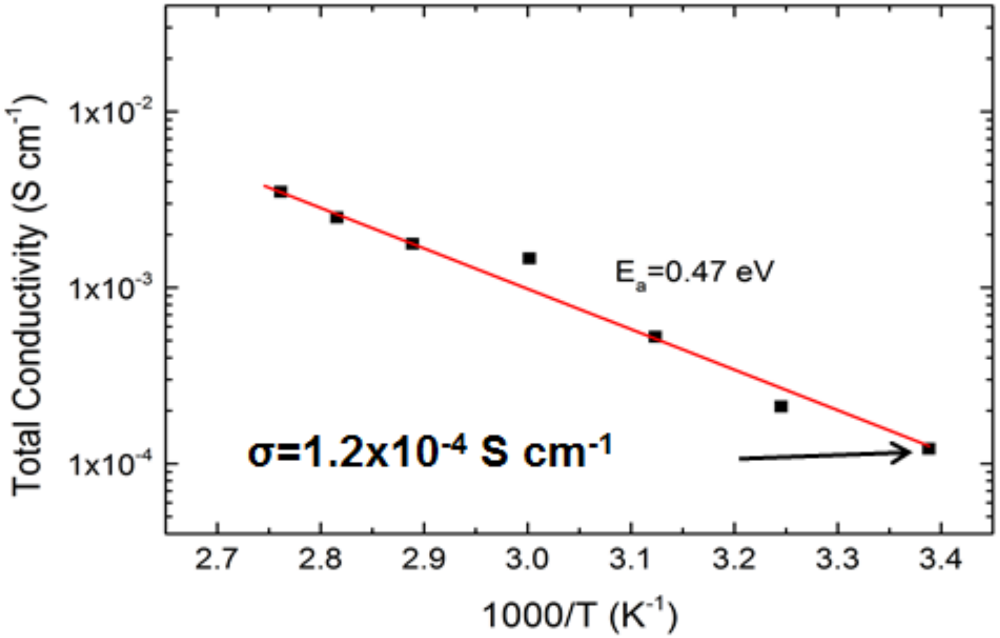

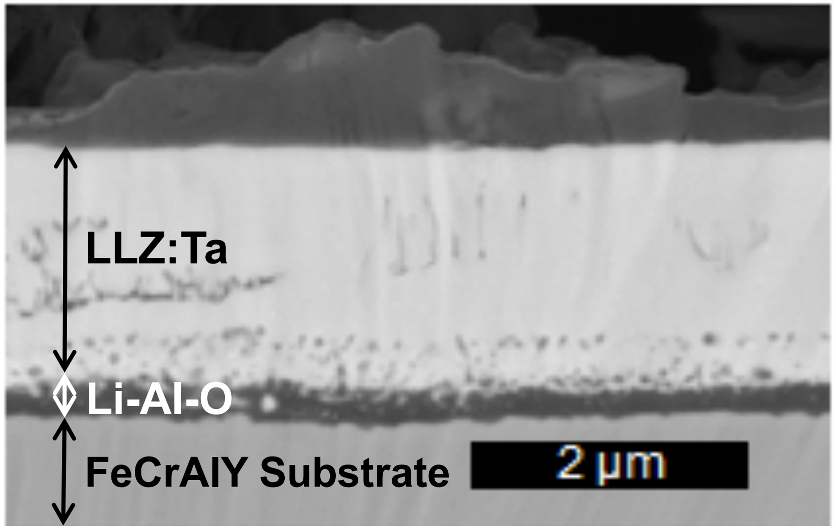

- Thickness: 2 µm
- Substrate temperature: >650° C
- Dense layer, cubic phase LLZ:Ta
- Total conductivity 1.2x10^{-4} S/cm at R.T.

S. Lobe, C. Dellen, M. Finsterbusch, H.G. Gehrke, D. Sebold, C.-L. Tsai, S. Uhlenbruck, O. Guillon
Journal of Power Sources 307 (2016) 684 - 689

PVD of LLZ:Ta – Advanced Li Analysis

JÜLICH
FORSCHUNGSZENTRUM

SIMS Profile

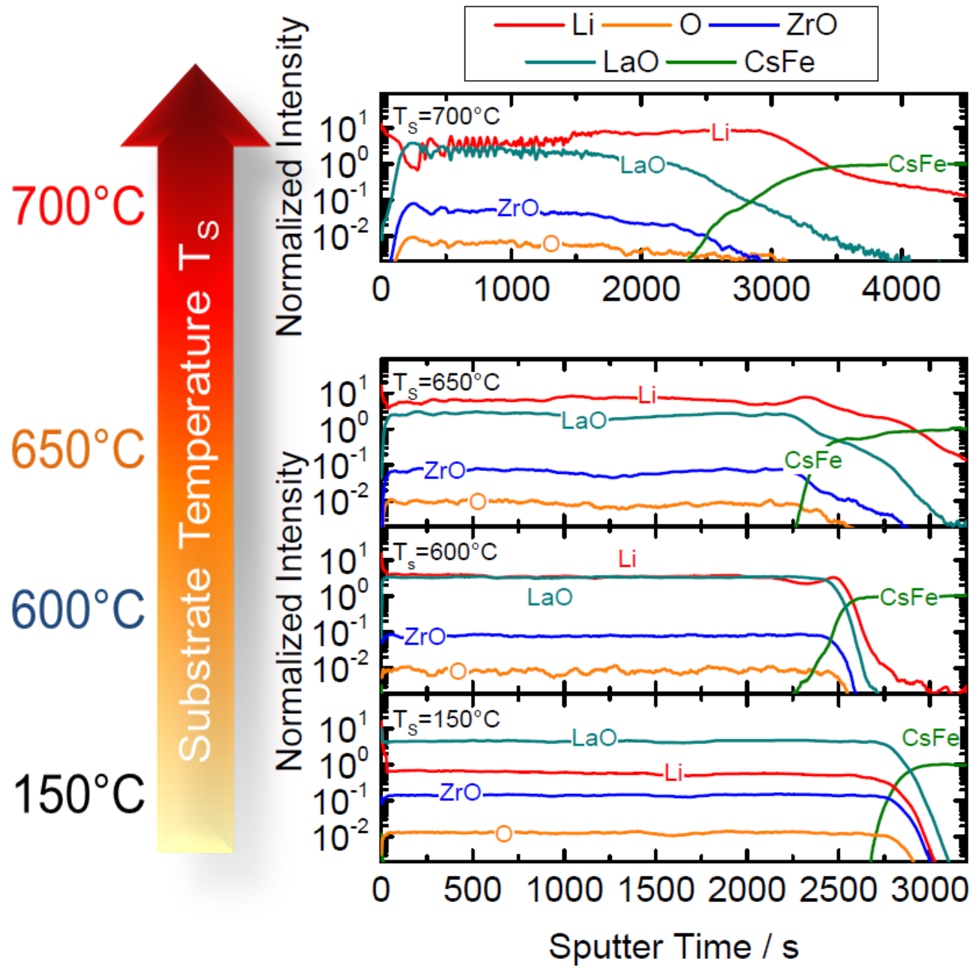

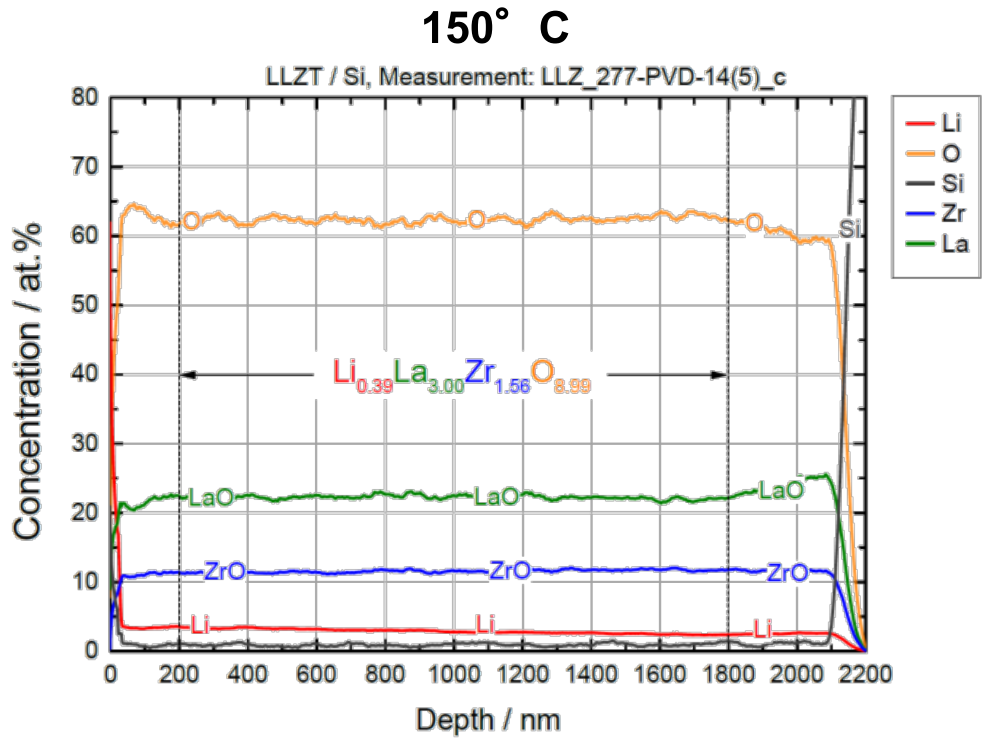

Method	Stoichiometry	ρ_{Li} [at./cm^3]
SIMS	$Li_{0.4}La_{3.0}Zr_{1.6}O_9$	1.66×10^{21}
NRA	$Li_{0.3}La_{3.0}Zr_{1.2}Ta_{0.1}O_{6.6}$	1.72×10^{21}
Sputter Target	$Li_{7.6}La_{3.0}Zr_{1.6}Ta_{0.4}O_{12.6}$	

Quantitative Li analysis with high resolution and 3D reconstruction is possible!

Compatibility Requirements of Electrode Material

- Chemically stable to solid electrolyte at sintering temperature, e.g.
  LLZ:Ta >1000 ° C
- Thermal expansion coefficient match to solid electrolyte
- Provide some Li-ion and electronic conductivity
- Low volume change during charge-discharge (<7.5%).

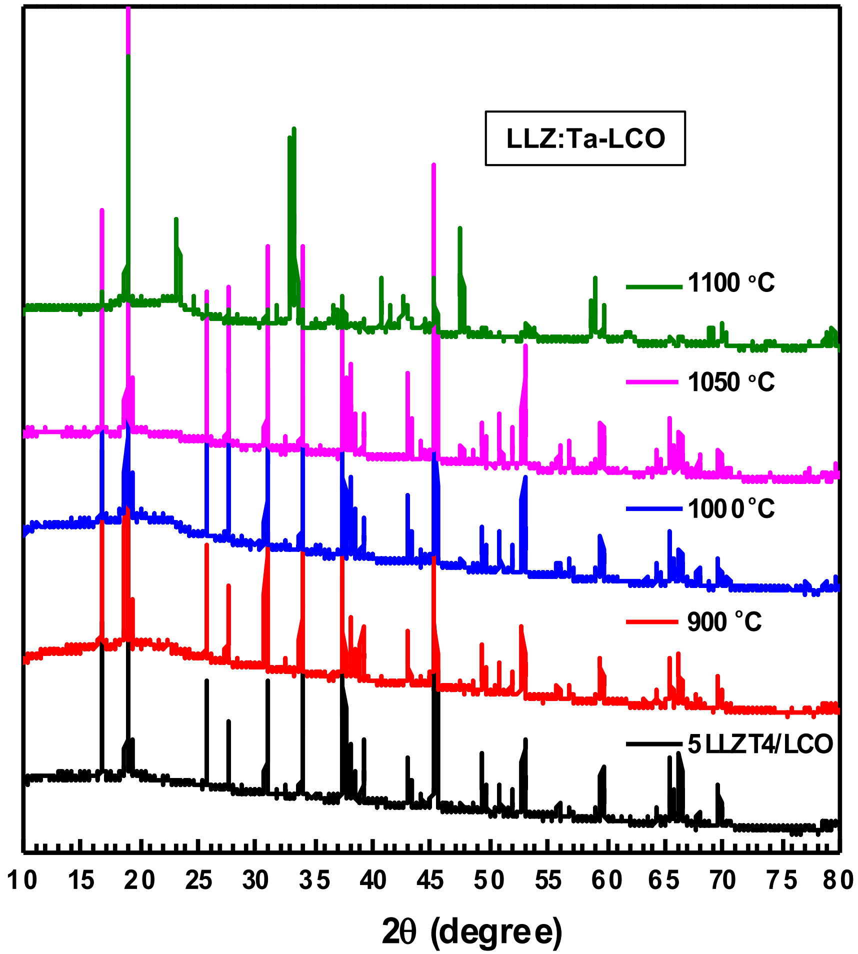

LLZ:Ta and $LiCoO_2$ have no major reaction up to 1085 °C

S. Uhlenbruck, J. Dornseiffer, S. Lobe, C. Dellen, C.-L. Tsai, B. Gotzen, D. Sebold, M. Finsterbusch, O. Guillon
J. Electroceramics, 2017

Cathode Microstructure and Battery Performance

Fabrication of "bulk" ASBs:

- Electrolyte supported cell
- Pure or mixed LCO cathode (Low T sintering)
- Li metal Anode

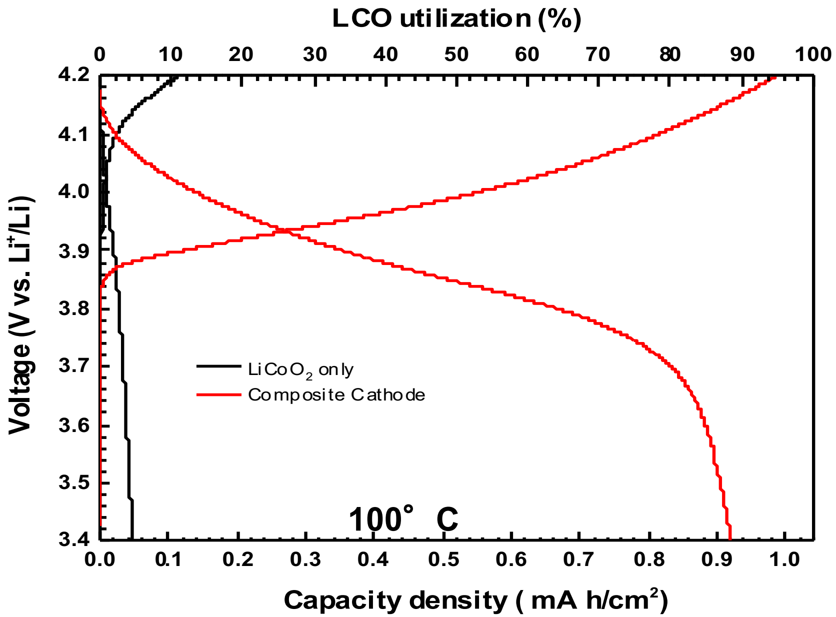

Galvanostatic voltage profile for both types of cathode

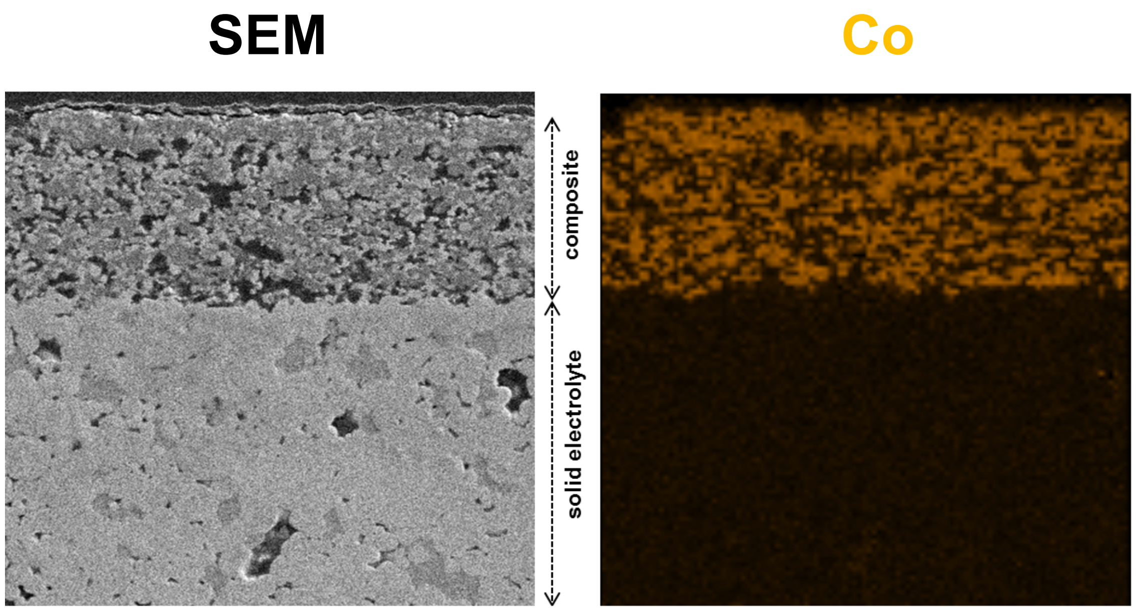

Microstructure of $LiCoO_2$ and LLZ:Ta composite cathode

Reversible Li extraction from LCO:

- Capacity (utilization) increase for mixed cathode
- High cathode porosity still challenging

Cathode Microstructure and Battery Performance

Volume fractions:

LCO	63%
LLZ	30%
Pores	7%

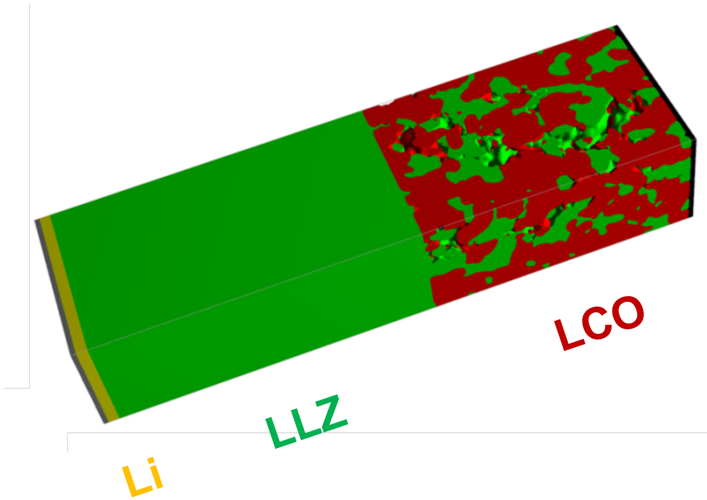

Battery and Electrochemistry Simulation Tool

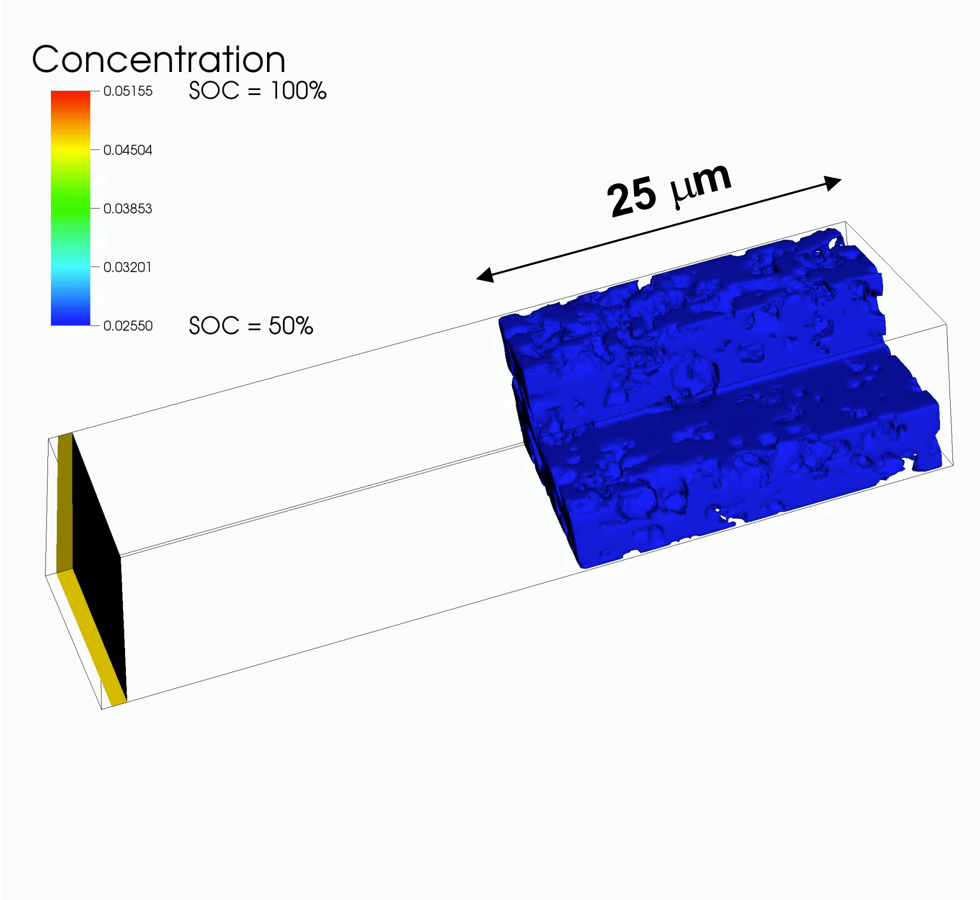

M. Finsterbusch, T. Danner, C.-L. Tsai, S. Uhlenbruck, A. Latz, O. Guillon, to be submitted, 2017

General conclusions

- Inorganic materials are key-enabler for future energy supply

- Ceramics have unique thermomechanical and electrochemical properties which can be widely tuned and optimized

- Final properties of a functional layer depend on its microstructure and thickness, which both depend on processing route and processing parameters

- Integration of materials into devices is a critical but necessary step between materials development and application

HI MS | HELMHOLTZ-INSTITUTE IONICS IN ENERGY STORAGE

JARA Jülich Aachen Research Alliance

JÜLICH FORSCHUNGSZENTRUM

Thank you for your attention!